J Neurophysiol 89: 40–56, 2003;
10.1152/jn.00272.2002.

Response Properties of Whisker-Associated Trigeminothalamic Neurons in Rat Nucleus Principalis

BRANDON S. MINNERY AND DANIEL J. SIMONS
Department of Neurobiology, University of Pittsburgh, Pittsburgh, Pennsylvania 15261

Submitted 12 April 2002; accepted in final form 20 August 2002

Minnery, Brandon S. and Daniel J. Simons. Response properties of whisker-associated trigeminothalamic neurons in rat nucleus principalis. *J Neurophysiol* 89: 40–56, 2003; 10.1152/jn.00272.2002. Nucleus principalis (PrV) of the brain stem trigeminal complex mediates the processing and transfer of low-threshold mechanoreceptor input en route to the ventroposterior medial nucleus of the thalamus (VPM). In rats, this includes tactile information relayed from the large facial whiskers via primary afferent fibers originating in the trigeminal ganglion (NV). Here we describe the responses of antidromically identified VPM-projecting PrV neurons ($n = 72$) to controlled ramp-and-hold deflections of whiskers. For comparison, we also recorded the responses of 64 NV neurons under identical experimental and stimulus conditions. Both PrV and NV neurons responded transiently to stimulus onset (ON) and offset (OFF), and the majority of both populations also displayed sustained, or *tonic*, responses throughout the plateau phase of the stimulus (75% of NV cells and 93% of PrV cells). Average ON and OFF response magnitudes were similar between the two populations. In both NV and PrV, cells were highly sensitive to the direction of whisker deflection. Directional tuning was slightly but significantly greater in NV, suggesting that PrV neurons integrate inputs from NV cells differing in their preferred directions. Receptive fields of PrV neurons were typically dominated by a "principal" whisker (PW), whose evoked responses were on average threefold larger than those elicited by any given adjacent whisker (AW; $n = 197$). However, of the 65 PrV cells for which data from at least two AWs were obtained, most (89%) displayed statistically significant ON responses to deflections of one or more AWs. AW response latencies were 2.7 ± 3.8 (SD) ms longer than those of their corresponding PWs, with an inner quartile latency difference of 1–4 ms ($\pm 25\%$ of median). The range in latency differences suggests that some adjacent whisker responses arise within PrV itself, whereas others have a longer, multi-synaptic origin, possibly via the spinal trigeminal nucleus. Overall, our findings reveal that the stimulus features encoded by primary afferent neurons are reflected in the responses of VPM-projecting PrV neurons, and that significant convergence of information from multiple whiskers occurs at the first synaptic station in the whisker-to-barrel pathway.

INTRODUCTION

The whisker-barrel pathway of the rodent trigeminal system is characterized at each level of the neuraxis by the presence of distinct cellular aggregates that correspond in a one-to-one fashion to the large vibrissae of the mystacial pad. Over the last several decades, anatomical and physiological studies of cortical barrels have yielded abundant insights into how the CNS processes sensory information (reviewed in Simons 1995). This scrutiny has also extended to subcortical stages of the whisker afferent pathway, where investigators have studied the responses of third-order neurons within thalamic "barreloids" (Armstrong-James and Callahan 1991; Simons and Carvell 1989), as well as the responses of primary afferent (first-order) neurons of the trigeminal ganglion (NV) (Gibson and Welker 1983a,b; Lichtenstein et al. 1990; Shoykhet et al. 2000; Zucker and Welker 1969). Far less is known, however, regarding the physiology of second-order neurons within the brain stem trigeminal complex.

In the rodent brain stem, whiskers are represented in cytochrome oxidase-rich patches termed "barrelettes," which are present in both nucleus principalis (PrV) and in two of the three subdivisions of the spinal trigeminal nucleus (SpV) (Belford and Killackey 1979; Durham and Woolsey 1984; Ma 1991; Ma and Woolsey 1984; Sikich et al. 1986). The barrelettes of PrV receive a dense innervation of low-threshold mechanoreceptor input from NV (Clarke and Bowsher 1962; Hayashi 1980; Jacquin et al. 1993), and in turn, provide the bulk of ascending afferents to the barreloids of the ventroposterior medial (VPM) thalamic nucleus (Bruce and McHaffie 1987; Chiaia et al. 1991; Erzurumlu et al. 1980; Peschanski 1984; Smith 1973; Veinante and Deschênes 1999; Williams et al. 1994). Previous studies have demonstrated a critical role for PrV in the relay of afferent information (Rhoades et al. 1987) and in the establishment of whisker-patterned somatotopy within VPM (Killackey and Fleming 1985). However, despite the importance of PrV in lemniscal transmission, few studies have examined in quantitative detail the response properties of trigeminothalamic PrV neurons.

Until relatively recently, a major handicap in the investigation of second-order trigeminal circuitry has been a poor understanding of the anatomical structure of PrV and of the synaptic wiring of its component cells. Nevertheless, a consensus has emerged that PrV mediates the processing of the fine spatial details of tactile stimuli within the ascending lemniscal pathway. In accordance with this notion, the majority of PrV cells have been shown to project to contralateral VPM, where their axon terminals ramify within dimensions consistent with the size of a single barreloid (Chiaia et al. 1991; Peschanski 1984; Veinante and Deschênes 1999; Williams et al. 1994). Recent studies have also shown that PrV neurons

Address for reprint requests: D. J. Simons, E 1440, Biomedical Science Tower, 200 Lothrop St., Univ. of Pittsburgh, Pittsburgh PA 15261 (E-mail: cortex@pitt.edu).

The costs of publication of this article were defrayed in part by the payment of page charges. The article must therefore be hereby marked "*advertisement*" in accordance with 18 U.S.C. Section 1734 solely to indicate this fact.

 0022-3077/03 $5.00 Copyright © 2003 The American Physiological Society

respond with high temporal fidelity to periodic whisker deflections (Ahissar et al. 2000; Sosnik et al. 2001). Understanding the sensory signal transmitted by PrV to VPM is a critical first step toward developing accurate models of thalamic function and will also be key to determining how second-order circuits themselves transform afferent information.

Of the few studies that have examined response properties of PrV neurons, most report that the majority of PrV cells respond phasically to deflections of only one whisker (Doherty et al. 1993; Jacquin et al. 1988; Shipley 1974; Veinante and Deschênes 1999; but see also Chiaia et al. 2000). The use of different types and levels of anesthesia, as well as differences in the nature of whisker stimuli, make it difficult to compare these reports with one another and with neuronal responses recorded in NV and VPM. The availability of directly comparable data sets for pre- and postsynaptic populations will greatly enhance our understanding of the role of PrV in processing afferent information and should enable the implementation of physiologically realistic models of thalamic circuitry (see for example Kyriazi and Simons 1993). Recently, Ahissar and colleagues have adopted such an approach for defining functional differences between whisker-associated neurons in the lemniscal and paralemniscal pathways (Ahissar et al. 2000; Sosnik et al. 2001).

The present study was motivated specifically by our ongoing interest in thalamic processing and more generally by our longer-term goal of developing realistic circuit models to account for response transformations at different levels of the whisker-barrel pathway. Here we describe quantitative receptive field properties of PrV and NV cells recorded under conditions identical to those of our previous investigations of thalamic and cortical neurons. We provide evidence that significant processing of afferent information occurs at the first synaptic station of the whisker-barrel pathway, and that the nature of the signal output from PrV to VPM is consistent with the known response properties of VPM neurons.

METHODS

Preparation for recording

PrV data were collected from adult female Sprague-Dawley rats weighing approximately 300 g. Animals were prepared for electrophysiological recordings using methods described previously in detail (Simons and Carvell 1989). In brief, a surgery was conducted under halothane anesthesia during which a tracheotomy was performed, the right jugular vein was catheterized, and a cannula was inserted into the left femoral artery. A steel post was then affixed to the skull for the purpose of stabilizing the head. This method was preferred to the use of a stereotaxic device in that it allowed unimpeded access to the whiskers and did not require the application of acute pressure points. Two small craniotomies were made in regions overlying the right ventrobasal thalamus and the anterior portion of the left brain stem trigeminal complex. Following surgery, animals were transferred to a vibration isolation table and were placed on a servo-controlled heating blanket. Halothane was discontinued and rats were maintained in a lightly narcotized state via a steady infusion of fentanyl delivered through the jugular catheter (Sublimaze, Jansen Pharmaceuticals; approximately 10 $\mu g \cdot kg^{-1} \cdot h^{-1}$). The responses of cortical barrel neurons (Simons and Land 1985; Simons et al. 1992) and thalamic barreloid neurons (Simons and Carvell 1989) recorded under light narcosis have been shown to be similar to those of awake or lightly anesthetized animals (Armstrong-James and Callahan 1991; Friedberg et al. 1999). To prevent spontaneous movements that occur with light narcosis, animals were immobilized by intravenous infusion of pancuronium bromide and were artificially respired for the remainder of the experiment. A computer continuously monitored femoral arterial blood pressure, heart rate, and tracheal airway pressure waveform. Core body temperature was maintained at 37°C.

NV data were collected from a separate group of rats (approximately 300 g). Surgical preparation and experimental procedures were the same as described above, with the exception that a craniotomy was made over the left NV. Previous studies of NV neurons in our laboratory have been carried out using sodium pentobarbital anesthesia and without neuromuscular blockade (Kyriazi et al. 1994; Lichtenstein et al. 1990; Shoykhet et al. 2000). However, to facilitate the explicit comparison of response parameters of populations of neurons separated by a single synapse (NV→PrV), we decided to acquire a new body of NV data under conditions identical to those from which PrV data were obtained.

Electrophysiological recordings

PRV/VPM. Coordinates for PrV and VPM were derived from the atlas of Pellegrino et al. (1979). Positioning the animal's head in the approximate plane of this atlas allowed us to advance the PrV recording electrode at an oblique angle through occipital cortex and thus enabled us to avoid damaging the transverse sinus located directly dorsal to PrV. Recording of single PrV neurons was accomplished using either stainless steel microelectrodes (500 kΩ–3 MΩ; Frederick Haer, Brunswick, ME) or low-impedance (approximately 500 kΩ) platinum-tungsten wire electrodes encased in quartz glass (Thomas Recording, Giessen, Germany). In VPM, receptive field (RF) mapping and antidromic stimulation were conducted through the same electrode, which in most experiments was a single, low-impedance stainless steel microelectrode (100–400 kΩ). In several earlier experiments, we employed a bipolar electrode comprised of two stainless steel microelectrodes cemented together with dental acrylic (tip separation approximately 300 μm).

During an experiment, the location of the recording electrode was inferred by the stereotyped somatotopy of the brain stem trigeminal nuclei (Jacquin et al. 1993). However, since the somatotopic map within PrV is continuous with that of the caudally adjacent subnucleus oralis (SpVo), it was often difficult to determine recording location based on this criterion alone. To address this problem we developed the following strategy. The first mapping penetration was made deliberately caudal to the suspected location of PrV so as to increase the likelihood that some portion of the trigeminal complex would be encountered. In subsequent penetrations, the electrode was advanced rostrally in approximately 300-μm increments until the anterior extent of the complex was surpassed, as was evidenced by a lack of responses to orafacial stimuli. At this point the electrode was repositioned several hundred micrometers caudal to the previous penetration. This last step usually ensured that we were recording in PrV. The successful evocation of antidromic spikes through electrical stimulation of contralateral VPM provided additional confirmation that the electrode was positioned within PrV, since SpVo projects only sparsely to thalamus and innervates primarily the posterior group (PO) (Jacquin and Rhoades 1990; Veinante et al. 2000). As was the case for the recording electrode, the location of the thalamic stimulating electrode was inferred through somatotopy (Land et al. 1995).

NV. The procedure for recording from NV cells has been described previously (Lichtenstein et al. 1990; Shoykhet et al. 2000). Although the details of our experimental preparation differ from those of earlier studies, the recording methods were the same and will not be fully recounted here. To summarize, the animal's head was positioned in the plane of the atlas of Paxinos and Watson (1998). High-impedance stainless steel microelectrodes (1–10 MΩ; Frederick Haer) were then used to isolate and record the responses of whisker-associated primary afferent neurons.

Antidromic identification of VPM-projecting neurons

We used antidromic stimulation of VPM in conjunction with a collision test protocol to identify VPM-projecting PrV neurons. Once the whisker representation in contralateral VPM was located (preferably a C, D, or E row barreloid), a search stimulus consisting of brief current pulses (0.05-ms duration, approximately 50 μA) was applied through the thalamic electrode while the recording electrode was simultaneously advanced through PrV. A spike occurring in response to thalamic stimulation was identified as potentially antidromic if it met the following criteria: *1*) constant latency response (<0.1 ms jitter; see Fig. 2*B*) at suprathreshold stimulation and *2*) the ability to follow a high-frequency stimulus. For the first criterion, latency was measured as the time between onset of the stimulus artifact and onset of the antidromic spike (Fig. 2*A*, *inset*). The second criterion was deemed satisfied if the recorded spike was able to follow twin stimulus pulses administered in brief (approximately 1 ms) succession. Putative antidromic spikes were then further isolated using a time/amplitude dual-window discriminator (BAK Electronics). After a spike was isolated, a collision test was performed in which the antidromic stimulus was triggered by the isolated PrV spike (Fig. 2*C*). A consistently successful collision between the spontaneously occurring PrV spike and the antidromic spike was taken as evidence that the isolated PrV cell was indeed a VPM-projecting neuron. All PrV cells described here met the criterion for a successful collision test. Although we often encountered cells that we were unable to activate antidromically, we did not conclude that these were non–VPM-projecting neurons, since the antidromic stimulus might simply have failed to depolarize all PrV axons terminating within the stimulated barreloid. For this reason we did not attempt to infer from negative findings the proportion of PrV cells that projected to VPM.

In one recent study of PrV projection neurons (Veinante and Deschênes 1999), it was suggested that antidromic stimulation of VPM may not be sufficient to distinguish VPM- projecting PrV cells from the minority of PrV projection neurons whose axons innervate the adjacent posterior group (PO) of the thalamus. Indeed, the broad-tipped bipolar stimulating electrodes (tip diameter approximately 50 μm; tip separation approximately 1 mm) employed in the aforementioned study may have been too large to ensure selective stimulation of VPM. We therefore chose to use single microelectrodes (tip diameter <5 μm) so that areas of high current density would be localized near the electrode tip during stimulation. In the several experiments in which we used a bipolar stimulating electrode, tip diameters were also small (<5 μm), and the tip separation (approximately 300 μm) was well within the dimensions of VPM. Although we did not systematically attempt to measure the spread of our antidromic stimulus currents, the small radius of the stimulus was evidenced by the fact that successful antidromic activation of PrV cells required close somatotopic alignment between stimulating and recording electrodes (i.e., no more than a 2-whisker disparity in alignment was usually allowable). Moreover, once an antidromic spike was isolated, subsequent movements of the stimulating electrode more than 200 μm in either direction along the dorsal-ventral axis typically resulted in the loss of the antidromic response even in cases where stimulating currents were set to well above threshold.

Histology

In the case of NV recordings, rats were administered a lethal dose of sodium pentobarbital at the conclusion of an experiment. Histological analyses were not conducted since the relative anatomical isolation of the ganglion precluded accidental recording of whisker-associated responses from nonprimary sources. Following PrV recording sessions, electrolytic marker lesions were made through both the PrV and VPM electrodes (7 μA for 7 s, anodal current). Animals were then deeply anesthetized with sodium pentobarbital and perfused transcardially. Brains were frozen, serially sectioned (60 μm) in an oblique coronal plane, reacted for cytochrome oxidase (CO), and counter-stained with thionin. Standard anatomical landmarks were used to determine the borders of VPM and PrV (Paxinos and Watson 1998), and tissue was visually inspected to confirm the presence of electrode tracks within the two nuclei (Fig. 1). Histological confirmation of PrV recording sites was successfully completed in all but 1 of 16 experimental animals (n = 3 cells). In a separate animal, procedural complications prevented reconstruction of electrode tracks in VPM (n = 3 cells). For these data, physiological criteria alone were used to determine recording/stimulation sites.

No attempt was made to correlate a PrV cell's response properties with its rostrocaudal location within the nucleus. Several cells located within the PrV/SpVo transition zone in caudal PrV were included in the present analyses and were presumed to be PrV neurons based on their projection target (VPM) and their physiological similarity to confirmed PrV cells. Occasionally electrode tracks were observed in rostral SpVo, but these typically corresponded to initial mapping penetrations which did not yield any data. Electrode tracks were never observed in the more caudal SpV subnuclei.

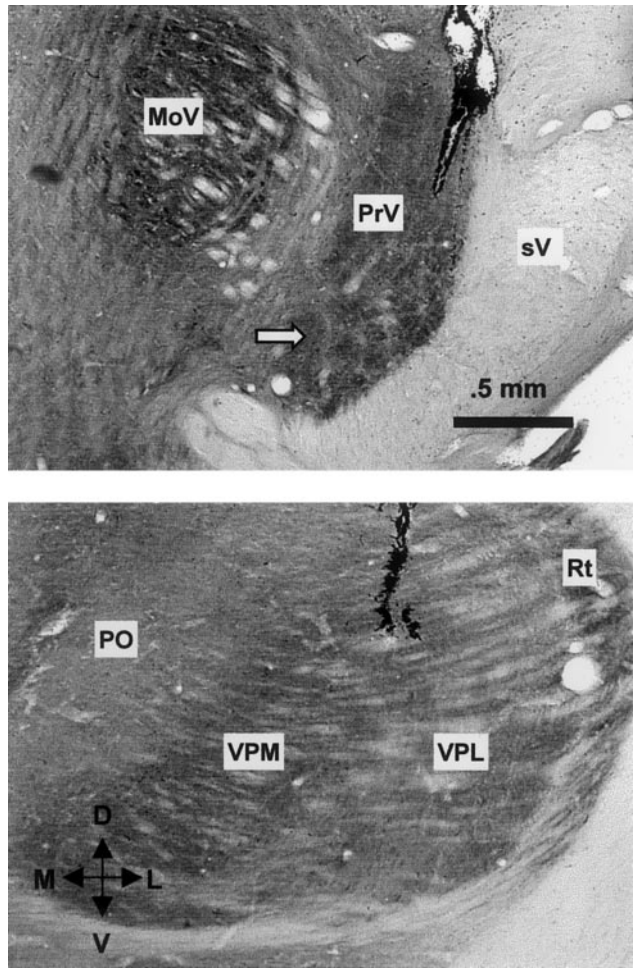

FIG. 1. Histological localization of electrode tracks in trigeminal nucleus principalis (PrV; *top*) and the ventroposterior medial nucleus of the thalamus (VPM; *bottom*) from a single experiment. Tissue sections (60 μm) were cut in an oblique coronal plane, reacted for cytochrome oxidase, and counter-stained with thionin. Electrode tracks are oriented dorsal-ventrally and are clearly visible in both nuclei. Note also the presence of barrelettes in ventral PrV (arrow). Abbreviations for anatomical landmarks are as follows: MoV, trigeminal motor nucleus; sV, sensory root of the trigeminal nerve; PO, posterior group; VPL, ventroposterior lateral nucleus; Rt, reticular nucleus.

Whisker stimulation

A hand-held probe was used to identify the whisker most effective at evoking activity in an isolated cell, i.e., the principal whisker (PW). A piezoelectric mechanical stimulator (Simons 1983) was then attached to the whisker approximately 10 mm from the skin surface. Ramp-and-hold stimulus waveforms were similar to those employed in previous studies in our laboratory and were generated via D/A converters using custom-written software in LabView (National Instruments, Austin, TX). Whisker deflections were applied 10 times in each of eight directions differing in 45° increments, for a total of 80 stimuli. Deflections were 1 mm in amplitude, with onset/offset velocities of 125 mm/s and a plateau duration of 200 ms. The angle of deflection was varied in a pseudorandom order throughout the stimulus presentation. This procedure was then repeated for several whiskers adjacent to the PW.

When possible, we recorded the responses of the rostral, caudal, ventral, and dorsal adjacent whiskers (AWs). Although in a few instances the surround component of a neuron's receptive field (RF) clearly extended beyond the four immediate AWs, we did not systematically investigate the responses of nonadjacent whiskers. For two PrV cells whose PW consisted of the Δ "straddler" whisker situated between rows D and E, only the dorsal AW (γ) response is described here. No straddler whiskers were included as AWs for any cell whose PW was not itself a straddler whisker. In the case where a cell responded robustly to multiple whiskers, the PW was taken to be the whisker that evoked the strongest response to stimulus onset averaged over all deflection angles.

The data collection protocol for a given cell typically lasted 25–40 min for PrV neurons and <10 min for NV neurons. Total recording sessions lasted 5–9 h for both NV and PrV recordings. This range does not include surgical preparation of the animal or time spent mapping the somatotopy of the respective nuclei, procedures that together required 5–7 h for PrV experiments, but no more than 5 h for NV experiments.

Data collection and analysis

All data in this study were derived from single-unit recordings. Spikes were isolated on-line by means of a time/amplitude dual-window discriminator. Many of the data analysis procedures used in this study have been described previously (Simons and Carvell 1989; Lichtenstein et al. 1990). Spike events were captured with 100-μs resolution and were compiled on-line into peristimulus time histograms (PSTHs) with 1-ms bin width. For each deflection angle, ON and OFF responses were calculated over a 20-ms window and were defined as the average number of spikes occurring in response to, respectively, stimulus onset and offset. Plateau responses were defined as the average number of spikes occurring within the middle 100 ms of the plateau epoch. Latencies to response onset were calculated from the total PSTH (all angles) and were defined as the earlier of two consecutive 1-ms bins in which the number of spikes significantly exceeded prestimulus firing rates ($P < 0.02$, assuming a Poisson distribution for prestimulus activity). All deflection angles were included in the PSTH since most neurons exhibited significant responses at multiple angles. In the case of many AW data files, no two consecutive bins met the criterion for significance for the ON and/or OFF window. These AWs were deemed unresponsive, and the corresponding files were excluded from subsequent analyses involving response latencies. All other AWs were classified as responsive. To test whether the criterion for two consecutive bins might have failed to detect a number of substantial yet very transient (i.e., <2-ms duration) responses, we examined the population PSTH for those AWs classified as unresponsive (ON and OFF PSTHs computed separately). Inspection of the PSTHs revealed that, as expected, responses were virtually absent, indicating that relatively few if any cells were misclassified as unresponsive.

For comparison with previous studies (Simons and Carvell 1989), we also tested for the presence of responses by comparing firing rates within the entire 20-ms response window to prestimulus firing rates estimated over a 100-ms period ($\alpha = 0.05$; 1-tailed *t*-test). This criterion proved slightly more liberal as it enabled the detection of broader, more temporally dispersed ON responses. The *t*-test method for detecting responses was used in this study to determine the number of "null angles" for a given cell, i.e., the number of deflection angles for which no responses were elicited.

Spontaneous activity levels for a given PrV cell were estimated using a 100-ms window of prestimulus activity collected from one of several AW data files for that cell. Approximately 50 ms separated the end of the prestimulus window from the beginning of stimulus onset. For reasons of consistency, the caudal AW was selected; but in cases where caudal AW data were absent, one of the other three AWs was substituted instead. We chose to use AW rather than PW data to calculate spontaneous activity since, due to the exquisite sensitivity of PrV cells, mere attachment of the stimulator to the PW often resulted in an elevation in spike discharges during the prestimulus period. For a number of PrV cells (38 of 72), we also recorded spontaneous firing rates by running the data collection protocol with the stimulator unattached to any whisker. Average spontaneous activity levels calculated using the latter method were nearly identical to those derived from AW prestimulus data. For NV, average spontaneous activity of the population was computed using data collected (stimulator unattached) from 50 of the 64 recorded cells.

A cell's adaptive properties were assessed through comparison of the plateau response with prestimulus activity measured over an equivalent period (Lichtenstein et al. 1990). If the plateau response at the maximally responsive angle exceeded prestimulus activity, the cell was classified as *tonic* (1-tailed *t*-test; $P < 0.025$). This criterion tended to be conservative because, as stated above, prestimulus activity occasionally yielded an inflated estimation of actual spontaneous firing rates. Those cells not classified as tonic were termed *phasic* by default.

Several analyses were used to characterize the degree to which PrV cells responded selectively to different deflection angles (i.e., directional tuning). The simplest of these, the *tuning ratio*, was calculated for each cell by dividing the mean ON response (averaged over all angles) by the ON response at the maximally responsive angle. In addition, we computed a *tuning index* for each neuron. Cells were categorized according to the number of deflection angles (0–7) that elicited a response that was statistically smaller than the maximum angle response ($P < 0.05$; 1-tailed *t*-test). To facilitate graphical comparison of directional tuning properties between populations, we also constructed normalized, rotated population polar plots. For a given population, each neuron's polar plot was first rotated so that maximally responsive angles were aligned for all cells. For a given cell, the response at each angle was normalized with respect to the maximum angle response for that cell, and average responses were then computed for each angle based on the whole population. All data analyses described above were implemented on an IBM PC using Microsoft Excel/Visual Basic software.

RESULTS

We recorded and analyzed the response properties of 72 whisker-associated, VPM-projecting PrV neurons in 16 fentanyl-sedated rats. Of our sample, the majority responded most robustly to stimulation of whiskers located within the ventral-most rows (rows D and E; 64 cells) and caudal-most arcs (arcs 1–3; 48 cells). Two cells had receptive field (RF) centers consisting of the Δ "straddler" whisker situated between rows D and E, caudal to arc 1. For the 72 PrV neurons described here, a total of 197 adjacent whisker (AW) responses were also recorded. In addition, we recorded the responses of 64 whisker-

associated trigeminal ganglion (NV) neurons in a separate group of four fentanyl-sedated rats. As was the case for the PrV recordings, the majority of NV data were collected from cells with RFs consisting of the large, caudal whiskers.

VPM-projecting PrV neurons were identified through antidromic stimulation of contralateral VPM (Fig. 1) and projection status was verified by means of a collision test (Fig. 2*C*; see also METHODS). All PrV data discussed hereafter were derived from confirmed VPM-projecting cells. Consistent with previous reports (Chiaia et al. 2000; Jacquin et al. 1988), the axons of PrV cells in our sample conducted rapidly, with an average antidromic latency of 0.89 ± 0.29 (SD) ms (see Fig. 2*A*). This value may in fact represent a slight underestimate given that our measurements did not take into account the delay between application of the antidromic stimulus and the evocation of an action potential (Takahashi 1965). Assuming an approximate point-to-point distance of 9 mm between ventral PrV and contralateral VPM (Paxinos and Watson 1998), average axonal conduction velocity for VPM-projecting PrV cells was approximately 10 m/s. No significant correlations were observed between conduction velocity and several of the standard response parameters we examined, including response magnitude and RF size.

Stimulus-evoked activity of PrV neurons

For each PrV cell, we identified the whisker that evoked the maximum excitatory response, termed that cell's "principal whisker" (PW). Figure 3*A* shows the response of a representative PrV neuron to ramp-and-hold deflections of its PW in eight directions differing in 45° increments. The firing rate for each deflection angle is represented in peristimulus time histograms (PSTHs). As was the case for the majority of our sample, the cell shown here responded transiently to both stimulus onset and offset (ON and OFF responses, respectively) and exhibited a sustained response during the plateau phase of the stimulus for deflections in at least one direction (compare Fig. 3*A* with the population response profile in Fig. 3*C*). ON and OFF responses were each determined using a 20-ms window, while plateau responses were calculated over the middle 100-ms period of the stimulus plateau (Fig. 3*C*). Note that, for the cell in Fig. 3*A*, ON response magnitudes on average exceeded those of OFF responses. This disparity between ON and OFF responses was observed often both in PrV and NV and is clearly seen in the PrV population PSTH (Fig. 3*C*). Response magnitudes for the cell in Fig. 3*A* also varied with deflection angle (Fig. 3*B*), a characteristic that is discussed in the following section. Distributions of response amplitudes at the maximally responsive angle for PW deflections ($n = 72$) are presented in Fig. 4 (*A–C*, dark bars), with ON, OFF, and plateau response epochs plotted separately. All recorded responses were included in the histograms irrespective of whether or not the criteria for statistical significance were met. Table 1 lists separately the means and SDs of statistically significant responses.

Comparison of activity: PrV versus NV

Spontaneous firing rates of PrV cells varied widely, but in most instances were great enough that the antidromic stimulus was not necessary to disclose the presence of a neuron. In

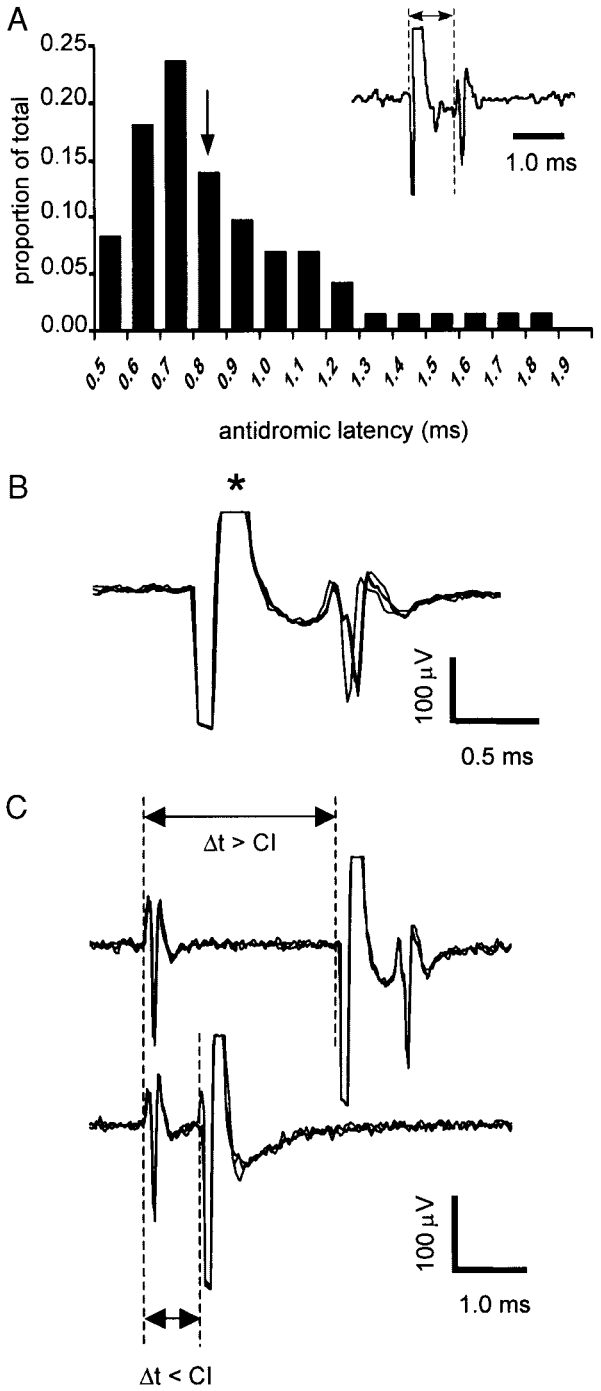

FIG. 2. Antidromic identification of VPM-projecting cells. *A*: distribution of antidromic latencies. Latencies were measured from the onset of the stimulus artifact to the onset of the antidromic spike (*inset*). Arrow above histogram indicates bin containing the mean antidromic latency for all cells ($n = 72$). *B*: 4 superimposed traces of an antidromic spike demonstrating small variability in latency. *Stimulus artifact. *C*: example of a collision test for the cell shown in *B*. *Top*: when the delay (Δt) between the spontaneously occurring spike and the antidromic stimulus was greater than the critical "collision interval" (CI), the spontaneous and antidromic spikes failed to collide. *Bottom*: when Δt was less than CI, the antidromic spike collided with the spontaneous spike and therefore did not appear following the stimulus artifact. CIs measured in this study were typically close to theoretical values as given by the formula: CI = antridromic latency + axonal refractory period. Axonal refractory periods were assessed using the twin pulse paradigm described in METHODS. (Note: 3 superimposed traces are shown for each scenario in *C*. Raw signals were high-pass filtered at 10 kHz to minimize the stimulus artifact.)

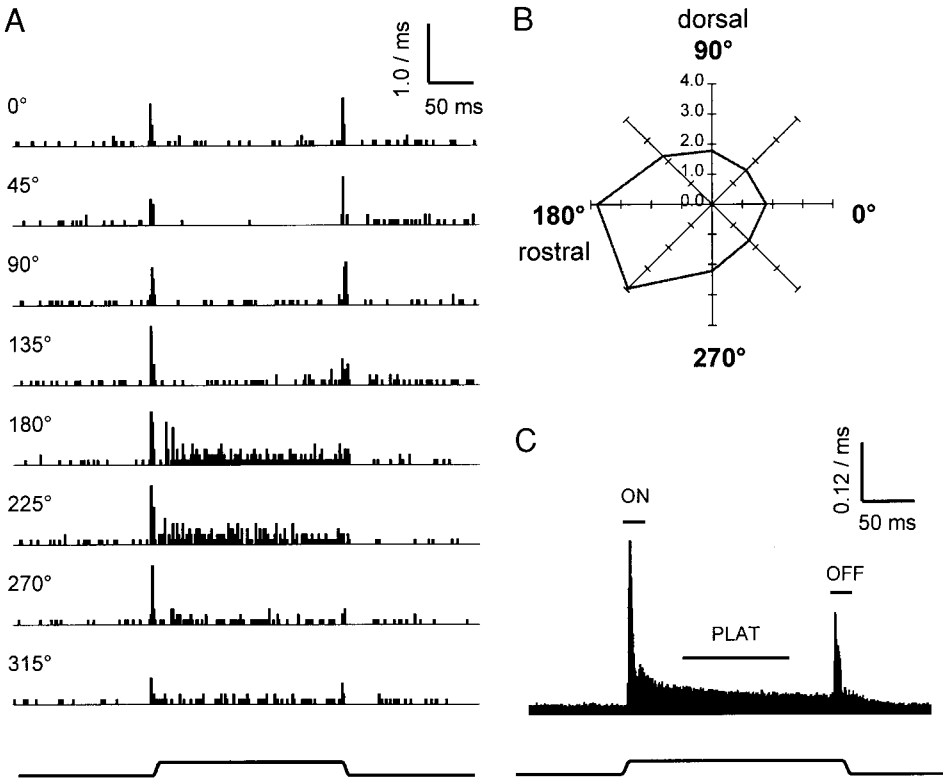

FIG. 3. Responses of VPM-projecting PrV neurons to ramp-and-hold deflections of the principal whisker (PW). *A*: peristimulus time histograms (PSTHs; 1-ms bins) showing response of a single PrV cell to PW deflections in 8 directions (10 trials per direction). Stimulus waveform is indicated at bottom. Units on vertical scale bar are spike probability per 1-ms bin (probability per bin = spikes per bin/number of trials). *B*: polar plot illustrating directional tuning of the cell shown in *A*. Units on axes are spikes per stimulus onset (ON). *C*: population PSTH for all VPM-projecting PrV cells ($n = 72$). Responses at all deflection angles are included in the PSTH (total deflections = 5,760). Horizontal bars indicate the 3 response windows from which subsequent data were derived. Scale bar units are same as in *A*.

contrast with earlier studies in deeply anesthetized rats, where PrV cells were described as relatively silent in the absence of peripheral stimuli (Jacquin et al. 1988; Kwan et al. 1999; Veinante and Deschênes 1999), mean spontaneous activity for our sample was 11.9 ± 12.6 Hz (Fig. 4*D*). To determine whether the high spontaneous firing rates of PrV cells might in part reflect input from NV, we recorded the spontaneous activity of 50 NV neurons (Fig. 4*D*). The mean spontaneous firing rate of the NV population, 6.9 ± 13.7 Hz, was less than that of PrV ($P < 0.001$; Mann-Whitney test), but greater than has been observed in previous NV studies conducted using sodium pentobarbital anesthesia without neuromuscular blockade (see DISCUSSION). It is therefore likely that afferent input from NV contributes to the high spontaneous firing rates of PrV cells observed under our experimental conditions.

Mean ON and OFF responses averaged over all deflection angles, although slightly greater in NV than in PrV, did not differ significantly ($\alpha = 0.05$) between the two populations (ON: $P = 0.15$; OFF: $P = 0.07$; Mann-Whitney test). However, maximum angle ON and OFF responses were on average larger in NV, whereas minimum angle ON and OFF responses were greater in PrV (see Table 1 for summary; all $P < 0.05$; Mann-Whitney test). In other words, the range of response magnitudes over all eight deflection angles was larger for NV neurons than for PrV neurons. To test the extent to which this finding was also reflected at the single-cell level, we computed for each neuron and each response window a coefficient of variation (CV) for responses over all eight angles. For both ON and OFF windows, CVs were greater for NV neurons ($P < 0.0001$ for both ON and OFF windows; Mann-Whitney test). As discussed in the following section, differences in response ranges between PrV and NV are reflected as differences in directional tuning between the two populations.

Inspection of PrV and NV population responses yielded readily observable differences in the shape of the PSTH for the ON and OFF responses. Figure 5 shows magnified population PSTHs for the maximally responsive ON (*left*) and OFF (*right*) angles. Also depicted is the temporal distribution of the NV-PrV response differential within the ON and OFF windows. The difference in maximum angle ON responses is notable in that, while the rise time and peak amplitudes were nearly identical for both populations, the NV ON response decayed gradually into the plateau phase of the response, whereas the PrV ON response declined rapidly following the initial several milliseconds. The source of the precipitous drop off in the PrV ON response is unclear, though it may involve rapid pre- and/or postsynaptic inhibition mediated by local GABAergic neurons within PrV (see DISCUSSION).

Directional tuning

In previous studies, whisker-associated primary afferent neurons in the rat were shown to possess a high degree of sensitivity to the direction of whisker deflection (Gibson and Welker 1983a; Lichtenstein et al. 1990; Zucker and Welker 1969). We explored the extent to which PrV responses reflect the directional selectivity of primary afferent inputs. Figure 6 shows that, like NV neurons, most PrV cells responded differentially based on deflection angle. To characterize directional tuning within the PrV population, we calculated a tuning ratio for each cell, defined as the ratio of the mean (all angles) ON response to the maximum angle ON response. Lower tuning ratios correspond to greater directional tuning. The distribution of tuning ratios for PrV is illustrated in Fig. 6*A* (0.61 ± 0.15). Of 72 PrV neurons, 20 (28%) had tuning ratios of 0.5 or less, indicating a maximum angle ON response that was at least double that of the average ON response.

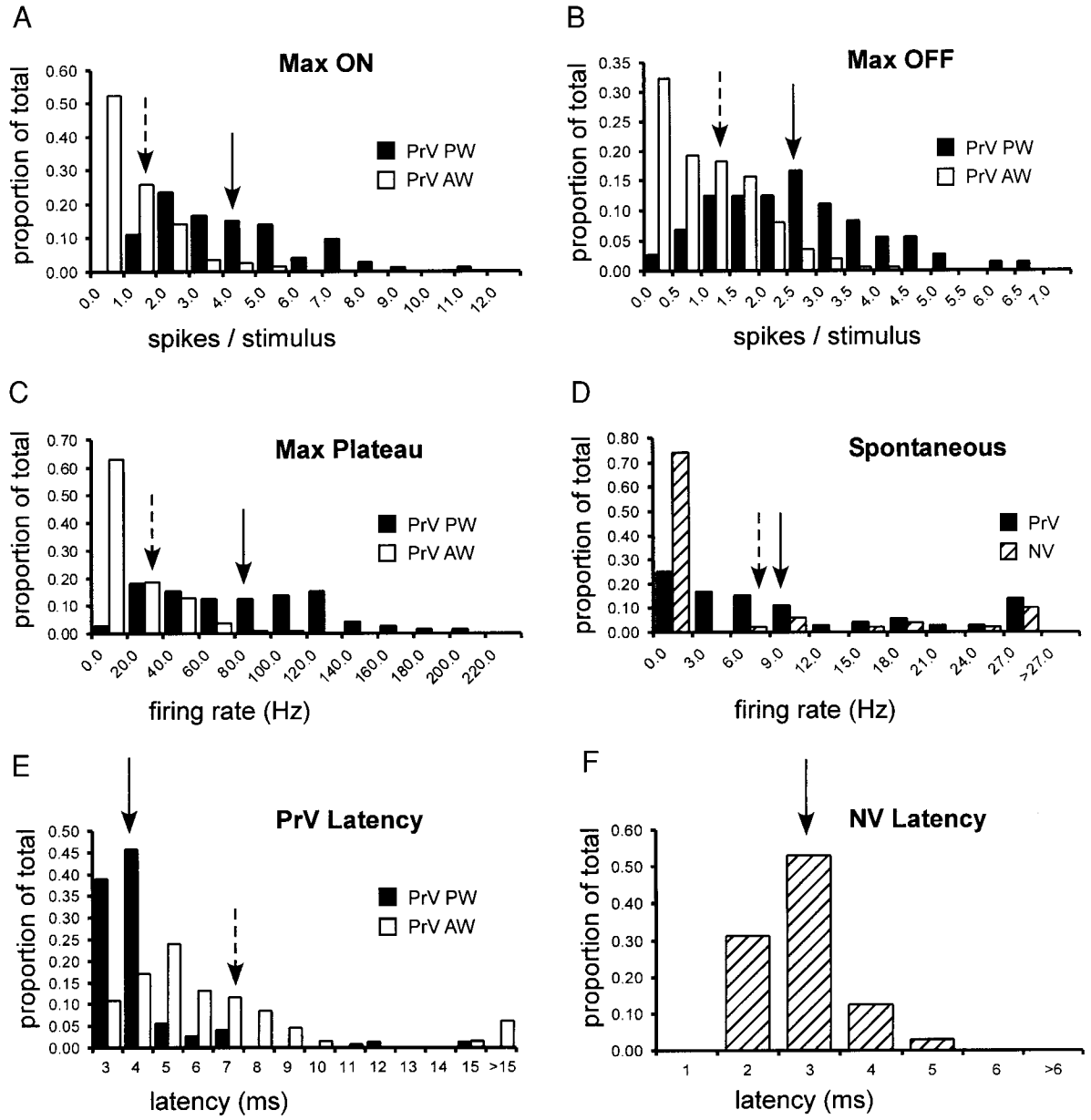

FIG. 4. Frequency distributions of stimulus-evoked/spontaneous activities and response latencies of VPM-projecting PrV cells. *A–C*: distributions of response magnitudes measured at each cell's maximally responsive deflection angle. All responses for all cells were included irrespective of statistical significance (PW, $n = 72$; AW, $n = 197$). Responses to stimulus onset (ON) and offset (OFF) were measured over 20-ms windows. Plateau responses were measured over the middle 100 ms of the stimulus plateau. All responses were averaged over 10 trials. *D*: distributions of spontaneous activity for PrV ($n = 72$) and trigeminal ganglion (NV, $n = 50$) populations. *E*: distributions of ON response latencies for PrV PWs and AWs. Latency to response onset for a given cell and a given whisker was calculated from the corresponding PSTH (all deflection angles included; see METHODS). Only statistically significant ON responses were included in the latency analysis (PW, $n = 72$; AW, $n = 129$). *F*: distribution of ON response latencies for NV neurons ($n = 64$). Latencies were calculated as in *E*. Temporal resolution for all latency measurements was 1 ms. Arrows over all histograms (*A–F*) indicate bins containing mean values (*A–C*: solid = PW, dashed = AW; *D*: solid = PrV, dashed = NV; *E*: solid = PW, dashed = AW; *F*: solid = NV).

We also computed a directional tuning index for each neuron (Fig. 6*B*). Cells were placed into one of eight categories (0–7) based on the number of angles having ON responses that were significantly less than the ON response at the maximally responsive angle $P < 0.05$; 1-tailed *t*-test). An index of 0 therefore represents a poorly tuned cell, whereas 7 indicates a highly tuned cell. The cell shown in Fig. 3*A*, for example, had a tuning index of 6. Nearly one-half of our sample (46%; 33 of 72 cells) was assigned an index of 6 or 7. Conversely, only 9 of 72 neurons (13%) were placed in the two lowest categories, 0 and 1. Despite the high variation in ON response magnitude across deflection angles for a given PrV cell, most angles typically exhibited statistically significant responses ($\alpha = 0.05$; 1-tailed *t*-test), and the mean number of angles that exhibited *no* response, termed "null angles," was small (1.33 ± 1.72). Also, although most PrV cells were directionally selective, mean responses at each angle averaged across all cells revealed no preference for a particular angle among the PrV population ($P > 0.7$; ANOVA).

TABLE 1. *Stimulus-evoked and spontaneous activities of PrV and NV neurons*

	PrV (n = 72)			
	PW (n = 72)	AW (n = 197)	AW*	NV (n = 64)
ON†				
Max	4.33 ± 2.21	1.30 ± 1.14	1.76 ± 1.14	5.64 ± 2.30
Min	1.31 ± 1.35	0.33 ± 0.59	0.48 ± 0.68	0.60 ± 0.93
All	2.65 ± 1.57	0.75 ± 0.83	1.05 ± 0.88	2.78 ± 1.28
OFF†				
Max	2.68 ± 1.32	1.13 ± 0.85	1.53 ± 0.80	3.56 ± 1.75
Min	0.79 ± 0.83	0.21 ± 0.37	0.30 ± 0.44	0.74 ± 1.13
All	1.70 ± 1.00	0.59 ± 0.55	0.82 ± 0.55	2.07 ± 1.31
Plateau‡				
Max	8.92 ± 4.42		3.70 ± 2.39	12.15 ± 7.87
Min	1.99 ± 2.43		1.42 ± 1.34	0.11 ± 0.39
All	5.00 ± 2.68		2.51 ± 1.89	4.61 ± 3.51
Spontaneous§	11.90 ± 12.70			6.90 ± 13.68

All values are means ± SD. PrV, nucleus principalis; NV, trigeminal ganglion; PW, principal whisker; AW, adjacent whisker; ON, onset; OFF, offset. * Includes only AWs that elicited statistically significant responses within the given window (ON: n = 129; OFF: n = 122). † Responses are defined as the average number of spikes occurring within the 20-ms response window (n = 10 deflections). "Max" and "min" refer to, respectively, maximally and minimally responsive deflection angles. "All" is the average of the mean response magnitudes for all angles (n = 8). ‡ Responses are the number of spikes occurring within the middle 100-ms period of the stimulus plateau. Only statistically significant (i.e., "tonic") responses are included (PW: n = 67; AW: n = 71; NV: n = 48). Responses were not adjusted for background activity. § Units are spikes/s.

Directional tuning of primary afferent responses was even more pronounced than in PrV. A larger percentage of NV neurons (55%; 35 of 64 cells) had directional tuning indices of 6 or 7 (Fig. 6*B*). Likewise, the average tuning ratio in NV was 0.51 ± 0.14 (see Fig. 6*A* for distributions), a value that was slightly but significantly less than that of the PrV population ($P < 0.001$; Mann-Whitney test). Compared with PrV, NV neurons also exhibited significantly more null angles (2.07 ± 1.89; $P < 0.01$; Mann-Whitney test). Figure 6*C* shows normalized, rotated population polar plots for NV and PrV (see METHODS). The sharper tuning of the NV population with respect to PrV is evident from the superposition of the two plots on the same axes. This difference in ON response tuning between the two populations was expected and reflects our earlier finding that the difference between maximum and minimal angle ON responses was on average less for PrV than for NV. Although OFF responses in PrV and NV also displayed clear directional selectivity, we did not conduct quantitative analyses of OFF response tuning (however, see Lichtenstein et al. 1990 for a discussion of OFF response tuning in NV).

For many well-tuned units, the preferred angle of deflection was independent of the position of the whisker at the onset of deflection. For example, a neuron that discharged vigorously to the *onset* of deflections in the caudal direction (0°) might also respond robustly to deflection *offsets* in the same direction, even though in the latter instance the whisker begins the movement from a rostrally deflected (180°) position. Such neurons are termed *directionally consistent* (Lichtenstein et al. 1990). As a measure of directional consistency, we computed for each cell a correlation coefficient (r) between the ON and OFF responses for all eight angles (n = 8; Fig. 7*A*). For a directionally consistent cell, the ON and OFF responses are inversely related, and r is therefore negative. Figure 7*B* shows the distribution of correlation coefficients for the PrV and NV populations (PrV: −0.26 ± 0.45; NV: −0.39 ± 0.52). Of the 72 PrV cells, 53 (74%) had negative correlation coefficients. However, like directional tuning, directional consistency for the PrV population was less pronounced than in NV ($P < 0.05$; Mann-Whitney test).

Population PSTHs further illustrate differences in directional consistency between NV and PrV. Figure 7*C* shows PSTHs for the angle evoking the maximum OFF response and for the angle opposite to it. Note that selecting for the angle opposite to the maximum OFF angle yields a comparatively larger ON response. This is to be expected if responses overall are directionally consistent, since the deflection offset at the angle evoking the maximum OFF response occurs in the same direction as the deflection onset at the opposite angle. Within NV this relationship was even more prominent than in PrV (compare *left* vs. *right* panel). Although little is known about the convergence ratio of NV inputs onto PrV neurons, our finding of broader directional tuning and less directional consistency within the PrV population is consistent with the notion that PrV cells integrate multiple inputs differing in their preferred directions.

Adaptive properties

Many studies of neurons along the whisker-barrel neuraxis have employed a binary, "tonic-versus-phasic" classification scheme for describing the adaptive properties of neuronal responses. Of our current sample of NV neurons, 75% (48 of 64 cells) were found to respond in slowly adapting, or *tonic*, fashion to whisker deflections. This percentage is identical to that recorded by Lichtenstein et al. (1990), using similar stimuli under different anesthetic conditions. The remaining pro-

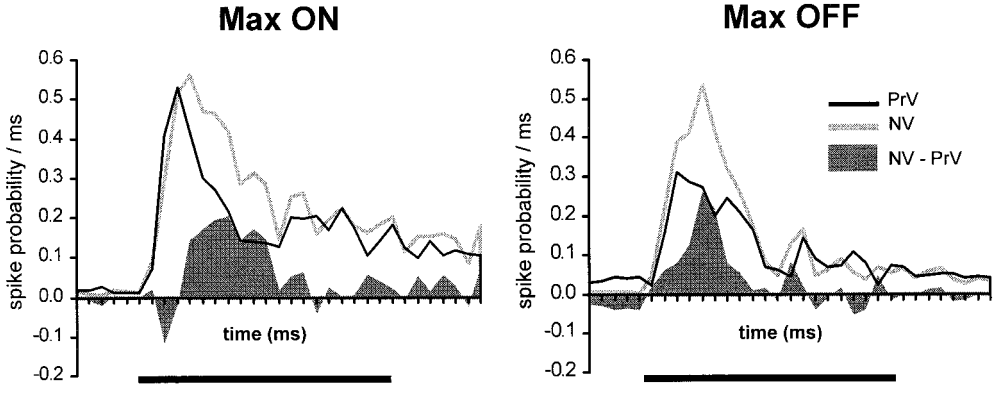

FIG. 5. Overlaid population PSTHs showing differences between VPM-projecting PrV neurons (black line, n = 72) and NV neurons (gray line, n = 64) in terms of maximum angle ON (*left*) and OFF (*right*) responses. Shaded area is the difference between the 2 populations (NV − PrV). Tick marks on x axis indicate 1-ms bins. Dark bars under each PSTH correspond to the 20-ms time window used to compute ON and OFF responses.

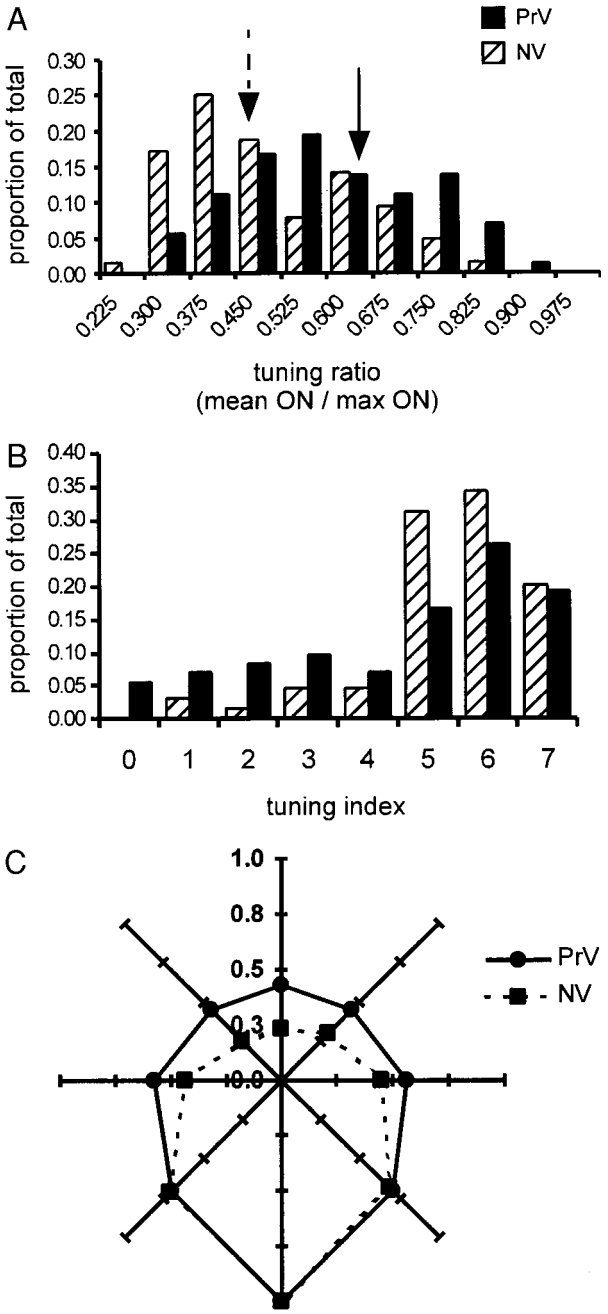

FIG. 6. Directional tuning of VPM-projecting PrV neurons ($n = 72$) compared with NV neurons ($n = 64$). All data shown (*A–C*) are for PW deflections. *A*: frequency distributions of tuning ratios, defined as [mean ON response (all angles)/maximum angle ON response]. Arrows indicate bins containing mean values (solid = PrV; dashed = NV). Note the stronger directional tuning of NV neurons as indicated by their smaller tuning ratios. *B*: distributions of directional tuning indices (see METHODS) for ON responses. Index of 7 indicates highly tuned response; 0 indicates lack of directional tuning. *C*: normalized and rotated population polar plots illustrating broader directional tuning of VPM-projecting PrV cells with respect to NV cells (see METHODS for description of how plots were constructed).

portion of cells within our sample, which responded only to the ON and OFF phases of the stimulus, were classified as rapidly adapting, or *phasic*, neurons. Tonic and phasic NV cells are known to differ along a number of parameters in addition to plateau response magnitude. In particular, phasic cells have less directionally tuned ON responses and exhibit less directional consistency (Gottschaldt et al. 1973; Lichtenstein et al. 1990). During our NV recording sessions, these differences were easy to recognize even without careful quantification. In the course of PrV recording sessions, however, it became apparent that such a clear dichotomy did not exist among PrV cells, as strictly phasic responses were virtually absent. When the tonic-phasic classification scheme (see METHODS) was applied to our sample of PrV neurons, a significantly larger percentage than in NV (93%; 67 of 72 cells) were found to respond tonically ($P < 0.005$; χ^2 test; see Fig. 8*A*).

The paucity of phasic neurons in PrV precluded meaningful tonic-versus-phasic comparisons for PrV responses. We therefore focused on comparing plateau responses between tonic NV and PrV populations. Despite a larger proportion of tonic PrV cells, we found that the maximum angle plateau responses of tonic neurons were on average weaker in PrV than in NV ($P < 0.05$; Mann-Whitney test; see also Table 1). This is evident from the population PSTHs in Fig. 8*B*, which show the background-subtracted, maximum angle plateau responses for the subpopulations of tonic NV and PrV cells. In contrast, *minimum* angle plateau responses were greater in PrV than in NV for tonic cells ($P < 0.001$; Mann-Whitney test; PSTHs not shown). Note that the pattern of plateau response differentials between NV and PrV parallels that described earlier for ON and OFF responses. As was the case for ON response tuning, the greater differential between maximum and minimum angle plateau responses in NV versus PrV suggests that the plateau responses of tonic PrV cells were less directionally tuned than their counterparts in NV. This disparity in tuning, which is evident in the population polar plots (Fig. 8*C*), is more pronounced than the difference in ON response tuning between NV and PrV (see Fig. 6*C*). The most parsimonious explanation for the broader plateau response tuning of tonic PrV cells is that these cells integrate multiple tonic inputs having slightly different preferred directions.

For each tonic cell in PrV and VPM, we also computed an adaptation index to assess the relative strength of the plateau response with respect to the ON response. The adaptation index was defined as a cell's maximum angle plateau response divided by its maximum angle ON response. Figure 8*D* shows the distributions of adaptation indices for NV and PrV. Despite the fact that both maximum angle ON and plateau responses differed between the two populations, adaptation indices were similar. Although the tendency was for PrV cells to have slightly greater indices than NV cells, this difference was not significant ($P = 0.11$; Mann-Whitney test).

Adjacent whisker responses

An important goal of the present study was to provide a quantitative description of the surround component of PrV RFs. For each PrV cell that we recorded, we applied our stimulus protocol successively to as many as four AWs. Of the 197 AWs tested, the majority resulted in statistically significant ON (65%; 129 AWs) and OFF (62%; 122 AWs) responses according to the criterion described in METHODS. Most PrV cells responded to deflections of one or more AWs. OF the 65 neurons for which data from at least two AWs were obtained, 58 (89%) exhibited statistically significant responses to deflections of at least one AW. However, average AW responses for all response windows were uniformly weaker than those of

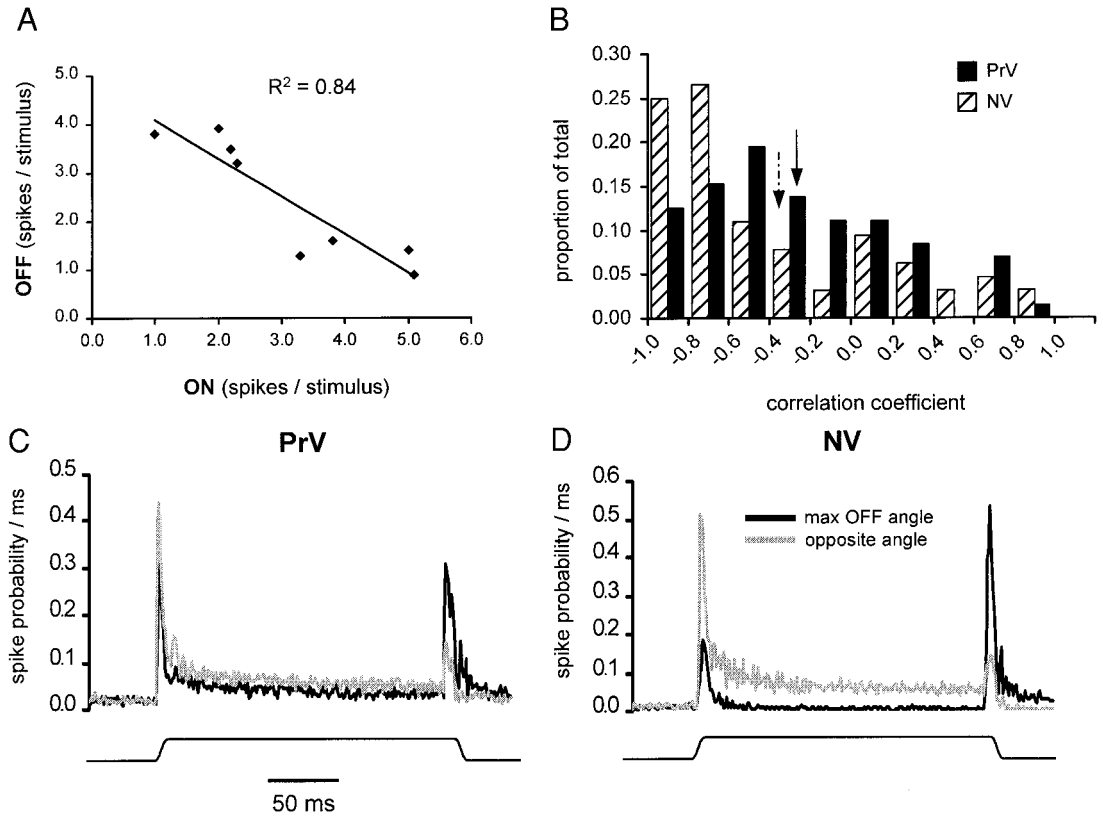

FIG. 7. Directional consistency of VPM-projecting PrV neurons (n = 72) vs. NV neurons (n = 64). *A*: scatter plot showing relationship between ON and OFF responses for a directionally consistent VPM-projecting PrV cell. The 8 points correspond to the 8 different deflection angles. OFF and ON response values for each point are averages of 10 deflections. *B*: distributions of correlation coefficients (OFF vs. ON) for both PrV and NV populations. Correlation coefficients were computed as shown in *A*. Arrows indicate bins containing mean values (solid = PrV; dashed = NV). Note the greater directional consistency of the NV population. *C*: population PSTHs demonstrating greater directional consistency of NV neurons (*right*) compared with VPM-projecting PrV neurons (*left*). Black line shows the population response at the angle producing the maximum OFF response. Gray line indicates the response at the opposite angle. Note that the tendency toward an inverse relationship between the 2 angles in terms of OFF: ON ratios is stronger in NV than in PrV.

PWs (Fig. 4, *A–C*, light bars; see also Table 1 for means and SDs). Differences in trial-by-trial variability between PW and AW responses were assessed by comparison of CVs calculated from maximum angle ON responses (n = 10 deflections). AW responses were found to exhibit considerably more variability than PW responses ($P < 0.0001$; Mann-Whitney test; data not shown). This finding was not unexpected, however, given that AW responses were overall much weaker than those of PWs and therefore were more likely to be influenced by fluctuations in background activity. Indeed, linear regression analysis showed a significant negative correlation between CV and ON response magnitude ($r^2 = 0.42$; $P < 0.0001$).

AW ON responses, when present, occurred on average at longer latencies than those of PWs (Fig. 4*E*). Mean latencies with respect to stimulus onset for PWs and AWs were, respectively, 4.1 ± 1.9 and 6.6 ± 4.0 ms ($P < 0.001$; Mann-Whitney test). By comparison, the mean response latency of NV neurons was 2.9 ± 0.8 (Fig. 4*F*). We also computed paired latency differences, i.e., the difference between each AW response and that of its corresponding PW. The average paired latency difference of 2.7 ± 3.8 ms ($P < 0.001$; Wilcoxon signed-rank test) was similar to the difference between the two population means (2.5 ms) reported above. The inner quartile range (±25% of median) for paired latency differences was 1–4 ms.

During recording sessions, it was apparent that a number of AW responses were not only statistically significant but were also quite robust relative to their corresponding PW responses. Figure 9*A* presents PSTHs for one cell in which multiple AWs elicited vigorous activity. To assess the relative strength of AW with respect to PW responses within the PrV population, we compared every AW response to that of its corresponding PW by calculating the ratio of their ON responses. The distribution of AW:PW ON response ratios is shown in Fig. 9*B* (0.29 ± 0.25). Of the 197 AWs stimulated, 41 (21%) evoked ON responses that were ≥50% that of their matched PW. However, approximately one-half (47%; 93/197) elicited responses that were ≤20% that of the corresponding PW. No relationship was found between the magnitude of a cell's PW ON response and its associated AW:PW ON response ratios. The distributions of AW:PW ON ratios for the four AWs are shown as cumulative probability plots in Fig. 9*C*. Mean values ± SD for the four whiskers were as follows: caudal, 0.32 ± 0.24; rostral, 0.31 ± 0.27; ventral, 0.30 ± 0.26; and dorsal, 0.23 ± 0.25. Although the dorsal AW evoked on average weaker responses relative to the PW than did the other whiskers, ANOVA revealed no significant differences among the four whiskers in terms of their AW:PW ON ratios ($P > 0.1$).

We next asked whether robust AW responses were distributed evenly across the population of PrV cells or whether they

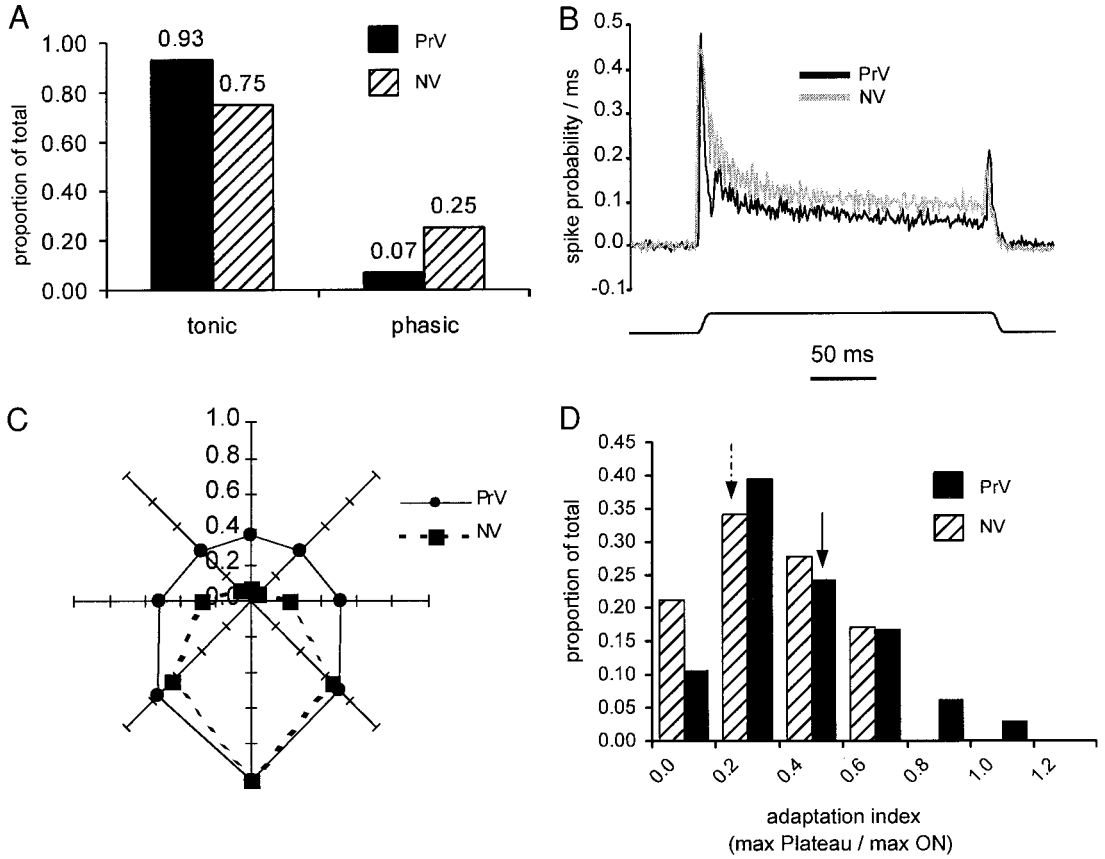

FIG. 8. Comparison of adaptive properties between VPM-projecting PrV neurons and NV neurons. *A*: proportion of cells in each population classified as tonic or phasic (see METHODS). Tonic cells responded during the plateau phase of the stimulus, while phasic cells responded only to the transient ON and/or OFF phases of the stimulus. *B*: overlaid, background-subtracted population PSTHs illustrating greater plateau responses of NV (gray line) neurons at the maximally responsive plateau angle. Only tonic NV ($n = 48$) and PrV (black line; $n = 67$) cells were included in the PSTHs. *C*: normalized and rotated population polar plots comparing directional tuning of plateau responses of tonic VPM-projecting PrV cells and tonic NV cells. Note the sharper tuning of plateau responses within the NV population. Polar plots were computed as described in METHODS. *D*: distributions of adaptation indices for tonic NV and PrV populations. Adaptation index was defined as the ratio of the maximum angle plateau response to the maximum angle ON response. Arrows indicate bins containing mean values (solid = PrV; dashed = NV).

were concentrated in a small subpopulation of our sample. We specifically examined those 65 PrV neurons for which data from at least two AWs had been collected. Of these, nearly one-half (49%; 32 cells) had at least one AW whose AW:PW ON ratio was >0.5. However, only nine cells (13%) had more than one AW with an AW:PW ON ratio >0.5. These findings indicate that the robust AW responses observed in our study were not confined to a small number of strongly multi-whisker cells, but instead were relatively common throughout PrV. Figure 9*D* shows the distribution of average AW:PW ON ratios for those 65 PrV neurons in our sample for which at least two AWs were tested (0.29 ± 0.20). Since the number and location (i.e., caudal, rostral, etc.) of tested AWs differed from cell to cell, for each cell we calculated the average AW:PW ON ratio using two randomly selected AWs. Although this approach necessitated the discarding of some AW data, it nevertheless offered the advantage of allowing us to include more cells in the distribution. Subsequent statistical analyses demonstrated that the distribution shown in Fig. 9*D* did not change significantly when additional AWs were included or when different AWs were used to compute the average AW:PW ON ratios (data not shown).

Comparison of responses: AW versus PW

We also investigated whether AW and PW responses differed with respect to parameters other than response magnitude and latency. A comparison of directional tuning properties between the two populations revealed that most AW ON responses, although somewhat less tuned than those of PWs, were nonetheless sensitive to stimulus direction (Fig. 10, *A* and *B*; cf. Figs. 10*A* and 6*B*). Likewise, when directional consistency was examined, the mean correlation coefficient (−0.33 ± 0.38) for AWs having both ON and OFF responses ($n = 107$) was found not to differ significantly from that of PWs ($P > 0.2$; Mann-Whitney test; distribution not shown). Another similarity between AW and PW ON response tuning was the lack of preference among the AW population for a particular angle ($P > 0.7$; ANOVA). This finding also held true when each of the four AW subpopulations (i.e., caudal, rostral, etc.) was examined separately (all $P > 0.15$; ANOVA). When individual AW ON response polar plots were compared with those of their corresponding PWs, no correlations in directional tuning were observed (average correlation coefficient, 0.11 ± 0.48), indicating that AW and PW inputs onto individual PrV cells are not matched for preferred direction.

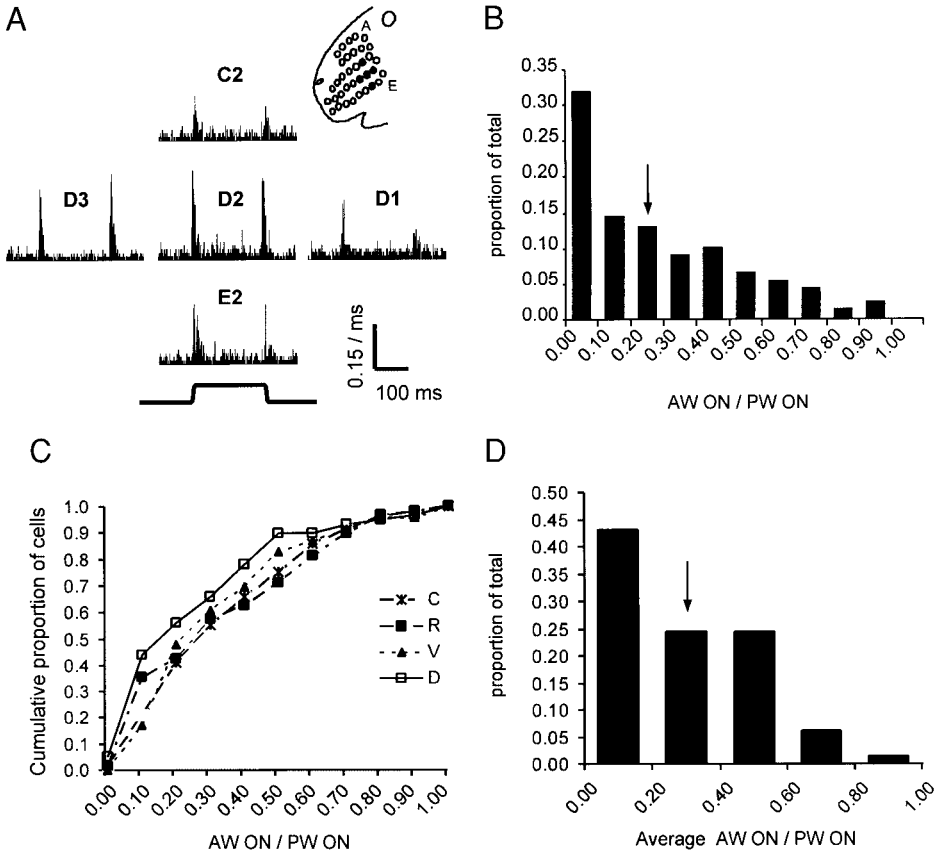

FIG. 9. Multi-whisker receptive fields of VPM-projecting PrV neurons. *A*: example of a VPM-projecting PrV cell that responded to stimulation of multiple adjacent whiskers (AWs). PSTHs are shown for the PW (D2) and the 4 AWs tested. *Inset*: location of whiskers on the face. Vertical scale bar is spike probability per 1-ms bin. *B*: distribution of AW:PW ON response ratios. Ratios were calculated by dividing each AW ON response ($n = 197$) by the ON response of the corresponding PW. Average (all angles) ON responses were used in the calculation of AW:PW ON ratios. Arrow indicates bin containing mean value. *C*: cumulative probability distributions of AW:PW ON response ratios for each of the 4 AWs tested. C = caudal ($n = 56$), *R* = rostral ($n = 59$), V = ventral ($n = 23$), D = dorsal ($n = 59$). *D*: distribution of average AW:PW ON response ratios for those PrV cells for which at least 2 AWs were tested ($n = 65$). Average AW:PW ON ratios for a given cell were calculated using 2 randomly selected AWs. Arrow indicates bin containing mean value.

Despite similarities in directional tuning, AW and PW responses differed markedly in terms of adaptive properties. Of those AWs that exhibited statistically significant ON responses, approximately 55% (71 of 129 AWs) also displayed significant plateau responses, i.e., were classified as tonic. Compared with the 93% of PW responses found to be tonic, the proportion of tonic responses was significantly lower for AWs ($P < 0.001$; χ^2 test). It is unclear from these findings, however, whether AW responses arise from disproportionately phasic input or whether tonic inputs are present but are differentially filtered with respect to more synchronous, transient (ON and OFF) responses.

DISCUSSION

We employed controlled whisker deflections to assess the response properties and receptive field characteristics of VPM-projecting PrV neurons. To understand how second-order cir-

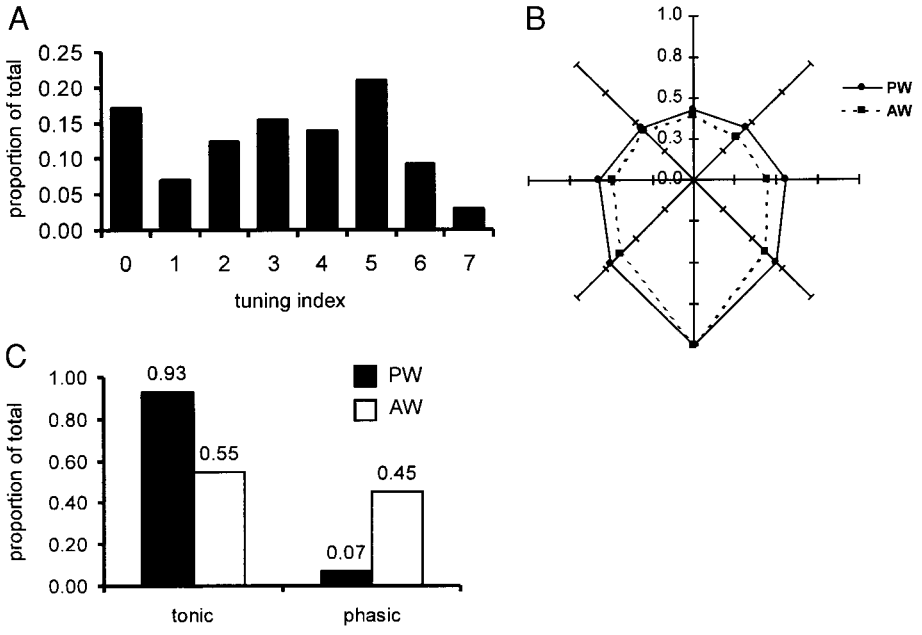

FIG. 10. Comparison of AW and PW response characteristics for VPM-projecting PrV neurons. *A*: distribution of directional tuning indices for statistically significant AW ON responses ($n = 129$). *B*: normalized and rotated population polar plots showing similarities between AW ($n = 129$) and PW ($n = 72$) ON response tuning. Polar plots were computed as described in METHODS. *C*: comparison of adaptive properties between AW and PW populations. Only AWs having statistically significant ON responses were included in the analysis.

cuits involving PrV transform afferent inputs, we also recorded the responses of whisker-associated NV neurons using the same stimuli applied under identical conditions. Our essential finding is that the encoded features of a tactile stimulus, as represented in NV responses, are for the most part preserved in the responses of VPM-projecting PrV cells. Overall response magnitudes were comparable in both populations, and both populations exhibited a high degree of directional tuning and a majority of tonic responses. However, response magnitudes occurred over a narrower range in PrV, a finding that was reflected in the broader directional tuning of PrV with respect to NV neurons. Both in NV and PrV, receptive fields were dominated by a single whisker. Unlike in NV, however, where neurons invariably possess single-whisker receptive fields (Gibson and Welker 1983a; Gottschaldt et al. 1973; Lichtenstein et al. 1990; Zucker and Welker 1969), numerous PrV cells responded to stimulation of adjacent whiskers, albeit with much lower firing rates than were elicited by PW stimulation.

Spontaneous activity

The present finding that PrV cells fire spontaneously at high rates is, as noted in the RESULTS, at odds with previous studies. In addition, NV spontaneous firing rates in the current report were considerably higher than those encountered in earlier experiments conducted in our laboratory under sodium pentobarbital anesthesia without neuromuscular blockade (Lichtenstein et al. 1990; Shoykhet et al. 2000). It is therefore likely that these discrepancies in spontaneous activity measurements are related to methodological differences between the present and earlier studies. For NV neurons in the current study, high spontaneous activity was almost exclusively associated with tonic cells. Moreover, it was often found that ongoing activity in these cells could be reduced or abolished by resetting the whisker's "neutral" position with a handheld probe. We interpret this to indicate that the ongoing activity of NV neurons was not wholly spontaneous in origin, but was in part due to sustained activation of tonic receptor endings while the whisker was supposedly in its neutral, or undeflected, position. (Note: while the same phenomenon was occasionally observed in PrV as well, the effect was less conspicuous and less prevalent than in NV.)

It appears that for the experimental preparation employed here, whiskers either drooped slightly from neutral position, or, when subjected to small displacements, did not rebound completely to their original, undeflected position. This phenomenon was most likely due to a loss of tone in mystacial pad musculature (Dorfl 1982) induced by neuromuscular blockade. Nevertheless, even under identical experimental conditions, spontaneous activity in PrV exceeded that of NV, suggesting that the ongoing activity observed in PrV arises in part from nonprimary sources. Stimulus-evoked responses of NV neurons reported here were also slightly larger than those recorded by Lichtenstein and colleagues without the use of pancuronium. Although we cannot rule out differences in anesthesia per se as the source of these discrepancies, it is reasonable to suppose that the mechanical properties of the facial tissue under pancuronium influence subtly the magnitude of primary afferent responses.

Response magnitude and tuning

Despite the finding that mean ON and OFF responses averaged over all deflection angles were slightly larger in NV than in PrV, these differences were not significant, indicating that afferent signal gain is not a major function of the second-order synapse. Interestingly, response magnitudes of individual PrV cells occurred within a narrower range, on average, than those of NV neurons. Several explanations are possible as to how PrV circuitry accomplishes this reduction in response range. The boosting of minimum angle responses, for instance, might be accounted for by the convergence onto individual PrV cells of inputs having different preferred directions. Our finding that fewer PrV responses exhibited "null" angles supports this contention. For example, a PrV neuron receiving input from two NV cells, each with a single, distinct null angle, would itself likely display no null responses, since afferent drive is provided at all deflection angles.

Inspection of maximum angle ON response PSTHs revealed that, following an initial rapid rise, the PrV response is rapidly truncated with respect to the NV response. GABAergic inhibition offers one possible mechanism by which second-order circuits might attenuate high-amplitude responses. Inhibition has been shown to influence responses of neurons in the rat dorsal column nuclei (Nunez and Buno 1999), and anatomical substrates for inhibitory interactions are known to exist also within PrV (Ginestal and Matute 1993; Haring et al. 1990; Lo et al. 1999). In the rat, Bae et al. (2000) showed that most NV terminals presynaptic to PrV cells are themselves recipients of axo-axonal GABAergic synapses. In addition, GABAergic synapses onto PrV dendrites postsynaptic to primary afferent terminals have been shown to occur frequently in the mouse (Xiang et al. 2000). A recent in vitro study by Lo et al. (1999) demonstrated that for a given barrelette cell, electrical stimulation of the trigeminal tract resulted in an excitatory postsynaptic potential followed immediately ($<$1 ms) by an inhibitory postsynaptic potential. This fast-onset inhibition is consistent with the rapid dip in ON response magnitude observed in the present study.

The onset time and duration of the PrV ON response suppression observed in our study are, however, notably shorter than the time course of GABA-mediated suppression of VPM responses, which occurs exclusively via feedback inhibition from the thalamic reticular nucleus (Rt) (reviewed in Guillery et al. 1998). In the latter case, suppression of VPM responses persists throughout the plateau phase, and sometimes results in the "phasic" classification of cells that, absent inhibition, would otherwise express tonic properties (Hartings and Simons 2000). Although PrV plateau responses are on average weaker than those of NV cells, the magnitude and duration of inhibitory interactions in PrV are apparently insufficient to mask the expression of statistically significant plateau responses.

One consequence of the decrease in response range from NV to PrV is that PrV cells exhibit broader directional tuning profiles than do NV cells. This fact not withstanding, most PrV cells in our study remained highly sensitive to the direction of deflection. Similarly, both Chiaia et al. (2000) and Veinante and Deschênes (1999) reported that the majority of VPM-projecting PrV cells in their respective samples responded selectively according to deflection angle. Although Jacquin et al. (1988) observed no directional tuning in labeled VPM-

projecting neurons, their sample size was small ($n = 10$), and tuning was not assessed through controlled stimuli or quantitative criteria. Other earlier studies are more difficult to compare with our own, since neuronal projection status was not identified. Nevertheless, most describe directionally tuned responses in PrV (Doherty et al. 1993; Kwan et al. 1999; Shipley 1974).

Adaptive properties

PrV receives both slowly (tonic) and rapidly (phasic) adapting inputs from NV, where the adaptive properties of primary afferent neurons are thought to reflect their specialized receptor endings at the periphery (Gottschaldt and Vahle-Hinz 1981; Gottschaldt et al. 1973; Rice et al. 1986). Previous studies have differed in their classifications of the adaptive properties of PrV cells, but most describe predominantly phasic responses. Shipley (1974) reported that in the anterior half of the trigeminal complex, 63% of cells responded in phasic fashion. Similarly, Veinante and Deschênes (1999), Jacquin et al. (1988), and Doherty et al. (1993) all reported a majority of phasic responses. In striking contrast, we found that more than 90% of VPM-projecting PrV neurons displayed tonic responses. Our results support the prevailing view that a major function of thalamic circuitry is the transformation of tonic input into phasic output via feedback inhibition from Rt (Gottschaldt et al. 1983; Hartings and Simons 2000; Lee et al. 1994a,b).

It is probable that the higher percentage of tonic PrV cells observed in our study is related in part to our stimulus regimen and to our statistical classification criteria. By deflecting whiskers in eight different directions, we are unlikely to have overlooked plateau responses that were directionally tuned to a small number of deflection angles. Also, the use of a quantitative classification scheme (see METHODS) led us to identify as tonic a number of cells whose plateau responses were otherwise difficult to discern via the audio monitor alone. Chiaia et al. (2000), who also used controlled, multi-angle deflections and quantitative criteria to assess adaptive properties, found that a majority (57%) of VPM-projecting PrV cells responded in tonic fashion. Furthermore, during their recordings the investigators carefully monitored vital signs to ensure that anesthetic doses were no greater than were required to maintain analgesia. The similarity between their findings and those recorded in fentanyl-sedated animals suggests that deeper levels of anesthesia, such as those employed in earlier studies, may mitigate the expression of sustained responses in PrV and therefore result in the classification of a larger percentage of neurons as phasic.

Unlike in some species, where tonic and phasic channels remain segregated along the afferent pathway (Dykes et al. 1981; Poggio and Mountcastle 1963; Powell and Mountcastle 1959), it is not known whether similar separation is maintained in the rodent trigeminal system. Detailed studies of the central terminals of whisker-associated primary afferent collaterals differing in adaptive properties have shown that this quality does *not* predict the distribution of synapses within rat PrV (Jacquin et al. 1993; Shortland et al. 1995, 1996). It is therefore unclear whether or to what extent phasic and tonic primary afferents converge onto individual PrV cells. The large percentage of tonic responses within PrV makes plausible the argument that at least some of those PrV cells that receive tonic NV input also receive input from phasic NV cells. Indeed, the broader directional tuning and less pronounced directional consistency of PrV responses with respect to those of NV could be explained by a widespread contribution of phasic NV inputs, which, compared with tonic NV responses, are less directionally tuned and less directionally consistent (see RESULTS for references). An alternative explanation is that these differences between PrV and NV responses result from the convergence within PrV of multiple, directionally consistent, tonic NV inputs differing in their preferred directions. This latter hypothesis does not require convergence of tonic and phasic inputs onto individual second-order neurons. Ultimately, simultaneous recordings from synaptically coupled pairs of NV and PrV neurons will be required to settle this question.

Multi-whisker receptive fields

Several groups reporting multi-whisker responses in VPM neurons have suggested that VPM receptive fields reflect input from multi-whisker trigeminothalamic neurons in SpV (Armstrong-James and Callahan 1991; Friedberg et al. 1999; Lee et al. 1994a; Rhoades et al. 1987). The most surprising result of the present study was that individual PrV neurons themselves provide multi-whisker inputs to thalamic barreloids. Nearly one-half of all VPM-projecting PrV neurons in our sample exhibited strong responses (defined as $\geq$50% of PW response) to stimulation of at least one whisker adjacent to the receptive field center. These findings contrast with those of earlier studies reporting a majority of single-whisker receptive fields in PrV (Doherty et al. 1993; Jacquin et al. 1988; Shipley 1974; Veinante and Deschênes 1999; but see also Chiaia et al. 2000).

It is conceivable that some of the antridromic responses in the present study may have resulted from accidental activation of PO-projecting PrV cells, whose axons frequently terminate near the PO/VPM border and whose receptive fields have been reported to include multiple whiskers (Veinante and Deschênes 1999). It is unlikely, however, that our sample was significantly contaminated by PO-projecting cells, as we employed fine-tipped stimulating electrodes to minimize current spread. As described in METHODS, the effective radius of our antidromic stimulus was likely small, since antidromic responses could be obtained only when the stimulating electrode in VPM and the recording electrode in PrV were in close somatotopic alignment. Despite these precautions, we cannot entirely rule out the occasional activation of PO-projecting axons traveling *en passant* through VPM (M. Deschênes, personal communication). Nevertheless, most previous reports agree that the large majority of cells in PrV project to VPM, with estimates ranging from approximately 70% (Veinante and Deschênes 1999) to approximately 90% (Chiaia et al. 1991). Thus even without the aid of antridromic stimulation, a random and unbiased sampling of neurons in PrV would reflect a majority of VPM-projecting cells. This suggests that, although antridromic stimulation of VPM may not have provided us with an entirely error-proof means of identifying VPM-projecting neurons, our resulting sample of antidromically identified cells most likely consists of an overwhelming majority of VPM-projecting neurons.

What then are the origins of the multi-whisker receptive fields of VPM-projecting PrV neurons? One possibility is that primary afferent inputs carrying sensory information from dif-

ferent whiskers converge onto the same PrV neuron. Although this explanation cannot be ruled out, Jacquin et al. (1993) showed that labeled NV axons tend to terminate within the histochemically defined boundaries of single barrelettes. Furthermore, dendritic fields of most barrelette neurons are small in the transverse plane, rendering them unlikely to sample adjacent whisker inputs from neighboring barrelettes (Jacquin et al. 1988; Lo et al. 1999; Ma 1991; Veinante and Deschênes 1999). Recurrent excitatory collaterals of PrV neurons provide an equally implausible explanation for multi-whisker responses, as they do not appear to exist in significant numbers in the rat (Jacquin et al. 1988; Veinante and Deschênes 1999). Perhaps the most likely source of adjacent whisker input derives from the dense network of intersubnuclear projections within the brain stem trigeminal complex itself. The majority of intersubnuclear fibers originate in the spinal trigeminal complex (SpV) and project both to PrV and to other SpV subnuclei (Jacquin et al. 1990a). Haring et al. (1990) demonstrated that none of the SpV neurons retrogradely labeled by tracer injections into PrV were immunoreactive for GABA or GAD, thus indicating that, at least in the case of PrV, intersubnuclear input serves an excitatory role. At present, no comprehensive study has investigated the contribution of SpV inputs to the receptive fields of trigeminothalamic projection neurons in PrV (but see Doherty et al. 1992).

The mean paired latency difference of 2.7 ms between adjacent and principal whisker responses is consistent with the notion that, at least in some cases, adjacent whisker input arrives via a long distance, multi-synaptic pathway. PrV receives input from each of the SpV subnuclei. The most caudal of these, subnucleus caudalis (SpVc), is located $\geq$3.5 mm caudal to PrV. The nearest SpV subnucleus, oralis (SpVo), lies in caudal continuity with PrV. It is therefore difficult to estimate a single intersubnuclear conduction time with which to compare our measured latency differences. The origin of adjacent whisker responses becomes even less clear when one considers that the modes of the adjacent and principal whisker latency distributions differed only by a millisecond (see Fig. 4*E*). Such a small difference could be accounted for by fast multi-synaptic transmission, but might also be explained by relatively longer integrative delays within PrV neurons of monosynaptic NV inputs from adjacent whiskers.

How do we reconcile our finding of multi-whisker responses in VPM-projecting PrV neurons with earlier reports of single-whisker receptive fields? The answer may lie in the anesthetic agent used in the present study. Under fentanyl-induced narcosis, animals were maintained on a lighter anesthetic plane than has been the case for previous PrV recordings conducted under sodium pentobarbital (Doherty et al. 1993; Jacquin et al. 1988; Shipley 1974), ketamine-xylazine (Chiaia et al. 2000; Veinante and Deschênes 1999), and urethane (Ahissar et al. 2000; Kwan et al. 1999). Investigations of the effects of anesthesia on the receptive field sizes of VPM neurons have shown that multi-whisker receptive fields are manifested at light anesthetic depths (Armstrong-James and Callahan 1991; Friedberg et al. 1999; Simons and Carvell 1989). However, it is presently unknown whether receptive fields of brain stem trigeminal neurons, like those of VPM, are affected by general anesthesia. Discrepancies in reported PrV receptive field sizes might also be due to the fact that most earlier studies failed to apply controlled stimuli and quantitative criteria in assessing adjacent whisker responses. To date, Chiaia et al. (2000) are the only other group to have measured the receptive fields of confirmed VPM-projecting PrV neurons by applying controlled deflections to individual whiskers outside the receptive field center. Overall receptive field sizes in the former study were found to be small, but were on average greater than one whisker (mean = 1.3 whiskers).

It is important to point out that our finding of multi-whisker receptive fields in PrV neurons should not be interpreted as a refutation of the prevailing hypothesis that PrV mediates the transmission of spatially precise information to the thalamus. Nor are our findings incompatible with those of other investigators reporting contrasting roles of lemniscal (PrV$\rightarrow$VPM) and paralemniscal (SpV$\rightarrow$PO) pathways in the processing of, respectively, the spatial and temporal features of a tactile stimulus (Ahissar et al. 2000). On average, principal whisker responses in our study were more than three times greater than those of their associated adjacent whiskers. Thus the spatial resolution of a PrV cell's receptive field was usually high despite the inclusion of significant surround components. In contrast, second-order thalamic projection neurons of the paralemniscal pathway, such as those of SpV subnucleus interpolaris, typically exhibit robustly multi-whisker receptive fields even at relatively deep levels of anesthesia (Jacquin et al. 1986, 1989; Veinante et al. 2000). Although single-whisker receptive fields have been observed in each of the three SpV subnuclei, these cells appear *not* to project substantially to the diencephalon (Veinante et al. 2000). What then is the role for multi-whisker receptive fields in lemniscal transmission? It is possible that the inclusion of adjacent whiskers in PrV receptive fields enables the dynamic regulation of spatial resolution in a behaviorally context-specific manner. This hypothesis is supported by the presence of extensive anatomical channels for higher-order control of trigeminothalamic transmission, both through corticobulbar inputs (Jacquin et al. 1990b) and through intersubnuclear pathways.

We are grateful to H. Kyriazi and A. Myers for expert technical assistance and to M. Deschênes for helpful discussions.

This work was supported by National Institute of Mental Health Grant MH-61372.

REFERENCES

Ahissar E, Sosnik R, and Haidarliu S. Transformation from temporal to rate coding in a somatosensory thalamocortical pathway. *Nature* 406: 302–306, 2000.

Armstrong-JamesM and Callahan CA. Thalamo-cortical processing of vibrissal information in the rat. II. spatiotemporal convergence in the thalamic ventroposterior medial nucleus (VPm) and its relevance to generation of receptive fields of S1 cortical "barrel" neurones. *J Comp Neurol* 303: 211–224, 1991.

Bae YC, Ihn HJ, Park MJ, Otterson OP, Moritani M, Yoshida A, and Yoshio S. Identification of signal substances in synapses made between primary afferents and their associated axon terminals in the rat trigeminal sensory nuclei. *J Comp Neurol* 418: 299–309, 2000.

Belford GR and Killackey HP. Vibrissae representation in subcortical trigeminal centers of the neonatal rat. *J Comp Neurol* 183: 305–321, 1979.

Bruce LL and McHaffie JGSBE. The organization of trigeminotectal and trigeminothalamic neurons in rodents: a double-labeling study with fluorescent dyes. *J Comp Neurol* 262: 315–330, 1987.

Chiaia NL, Rhoades RW, Bennett-Clarke CA, Fish SE, and Killacky HP. Thalamic processing of vibrissal information in the rat. I. Afferent input to the medial ventral posterior and posterior nuclei. *J Comp Neurol* 314: 201–216, 1991.

Chiaia NL, Zhang S, Crissman RS, and Rhoades RW. Effects of neonatal axoplasmic transport attenuation on the response properties of vibrissae-sensitive neurons in the trigeminal principal sensory nucleus of the rat. *Somatosens Mot Res* 17: 273–283, 2000.

ClarkeWB and Bowsher D. Terminal distribution of primary afferent trigeminal fibers in the rat. *Exp Neurol* 6: 372–383, 1962.

Doherty D, Jacquin MF, and Killackey HP. Quantitative analysis of receptive field properties in the rat nucleus principalis. *Soc Neurosci Abstr* 19: 327, 1993.

Doherty D, Killackey HP, and Jacquin MF. Receptive field synthesis in rat nucleus principalis: spinal trigeminal contributions. *Soc Neurosci Abstr* 18: 1190, 1992.

Dorfl J. The musculature of the mystacial vibrissae of the white mouse. *J Anat* 135: 147–154, 1982.

Durham D and Woolsey TA. Acute whisker removal reduces neuronal activity in barrels of mouse SmI cortex. *J Comp Neurol* 178: 629–644, 1978.

Dykes RW, Sur M, Merzenich MM, Kaas JH, and Nelson RJ. Regional segregation of neurons responding to quickly adapting, slowly adapting, deep and Pacinian receptors within thalamic ventroposterior lateral and ventroposterior inferior nuclei in the squirrel monkey (*Saimiri sciuresu*). *Neuroscience* 6: 1687–1692, 1981.

Erzurumlu RS, Bates CA, and Killackey HP. Differential organization of thalamic projection cells in the brainstem trigeminal complex of the rat. *Brain Res* 198: 427–433, 1980.

Friedberg MH, Lee SM, and Ebner FF. Modulation of receptive field properties of thalamic somatosensory neurons by the depth of anesthesia. *J Neurophysiol* 81: 2243–2252, 1999.

Gibson JM and Welker WI. Quantitative studies of stimulus coding in first-order vibrissa afferents of rats. 1. Receptive field properties and threshold distributions. *Somatosens Res* 1: 51–67, 1983a.

Gibson JM and Welker WI. Quantitative studies of stimulus coding in first-order vibrissa afferents of rats. 2. Adaptation and coding of stimulus parameters. *Somatosens Res* 1: 95–117, 1983b.

Ginestal E and Matute C. Gamma-aminobutyric acid-immunoreactive neurons in the rat trigeminal nuclei. *Histochemistry* 99: 49–55, 1993.

Gottschaldt K-M, Iggo A, and Young DW. Functional characteristics of mechanoreceptors in sinus hair follicles of the cat. *J Physiol (Lond)* 235: 287–315, 1973.

Gottschaldt K-M and Vahle-Hinz C. Merkel cell receptors: structure and transducer function. *Science* 214: 183–186, 1981.

Gottschaldt KM, Vahle-Hinz C, and Hicks TP. Electrophysiological and microphar macological studies on mechanisms of input-output transformation in single neurones of the somatosensory thalamus. In: *Somatosensory Integration in the Thalamus,* edited by Macchi G, Rustioni A, and Spreafico R. Amsterdam: Elsevier, 1983, p. 199–216.

Guillery RW, Feig SL, and Lozsadi DA. Paying attention to the thalamic reticular nucleus. *Trends Neurosci* 21: 28–32, 1998.

Haring JH, Henderson TA, and Jacquin MF. Principalis- or parabrachial-projecting spinal trigeminal neurons do not stain for GABA or GAD. *Somatosens Mot Res* 7: 391–397, 1990.

Hartings JA. *Somatosensory Processing in Inhibitory Feedback Circuits of the Thalamus* (PhD thesis). Pittsburgh, PA: University of Pittsburgh, 2000.

Hartings JA and Simons DJ. Inhibition suppresses transmission of tonic vibrissa-evoked activity in the rat ventrobasal thalamus. *J Neurosci* 20: RC100, 2000.

Hartings JA, Temereanca S, and Simons DJ. High responsiveness and direction sensitivity of neurons in the rat thalamic reticular nucleus to vibrissal deflections. *J Neurophysiol* 83: 2791–2801, 2000.

Hayashi H. Distributions of vibrissae afferent fiber collaterals in the trigeminal nuclei as revealed by intra-axonal injection of horseradish peroxidase. *Brain Res* 183: 442–446, 1980.

Jacquin MF, Barcia M, and Rhoades RW. Structure-function relationships in rat brainstem subnucleus interpolaris: IV. Projection neurons. *J Comp Neurol* 282: 45–62, 1989.

Jacquin MF, Chiaia NL, Haring JH, and Rhoades RW. Intersubnuclear connections within the rat trigeminal brainstem complex. *Somatosens Mot Res* 7: 399–420, 1990a.

Jacquin MF, Golden J, and Panneton WM. Structure and function of barrel 'precursor' cells in trigeminal nucleus principalis. *Dev Brain Res* 43: 309–314, 1988.

Jacquin MF, Mooney RD, and Rhoades RW. Morphology, response properties, and collateral projections of trigeminothalamic neurons in brainstem subnucleus interpolaris of rat. *Exp Brain Res* 61: 457–468, 1986.

Jacquin MF, Renehan WE, Rhoades RW, and Panneton WM. Morphology and topography of identified primary afferents in trigeminal subnuclei principalis and oralis. *J Neurophysiol* 70: 1911–1936, 1993.

Jacquin MF and Rhoades RW. Cell structure and response properties in the trigeminal subnucleus oralis. *Somatosens Mot Res* 7: 265–288, 1990.

Jacquin MF, Wiegand MR, and Renehan WE. Structure-function relationships in rat brain stem subnucleus interpolaris. VIII. Cortical inputs. *J Neurophysiol* 64: 3–27, 1990b.

Killackey HP and Fleming K. The role of the principal sensory nucleus in central trigeminal pattern formation. *Brain Res* 354: 141–145, 1985.

Kwan CL, DeMaro JA, Hu JW, Jacquin MF, and Sessle BJ. C-fiber depletion alters response properties of neurons in trigeminal nucleus principalis. *J Neurophysiol* 81: 435–446, 1999.

Kyriazi HT, Carvell GE, and Simons DJ. OFF response transformations in the whisker/barrel system. *J Neurophysiol* 72: 392–401, 1994.

Kyriazi HT and Simons DJ. Thalamocortical response transformations in simulated whisker barrels. *J. Neurosci* 13: 1601–1615, 1993.

Land PW, Buffer SA Jr, and Yaskosky JD. Barreloids in adult rat thalamus: three dimensional architecture and relationship to somatosensory cortical barrels. *J Comp Neurol* 355: 573–588, 1995.

Lee SM, Friedberg MH, and Ebner FF. The role of GABA-mediated inhibition in the rat ventral posterior medial thalamus. I. Assessment of receptive field changes following thalamic reticular nucleus lesions. *J Neurophysiol* 71: 1702–1715, 1994a.

Lee SM, Friedberg MH, and Ebner FF. The role of GABA-mediated inhibition in the rat ventral posterior medial thalamus. II. Differential effects of GABAa and GABAb receptor antagonists on responses of VPM neurons. *J Neurophysiol* 71: 1716–1726, 1994b.

Lichtenstein SH, Carvell GE, and Simons DJ. Responses of rat trigeminal ganglion neurons to movements of vibrissae in different directions. *Somatosensory Mot Res* 7: 47–65, 1990.

Lo FS, Guido W, and Erzurumlu RS. Electrophysiological properties and synaptic responses of cells in the trigeminal principal sensory nucleus of postnatal rats. *J Neurophysiol* 82: 2765–2775, 1999.

Ma PM. The barrelettes—architectonic vibrissal representations in the brainstem trigeminal complex of the mouse. I. Normal structural organization. *J Comp Neurol* 309: 161–199, 1991.

Ma PM and Woolsey TA. Cytoarchitectonic correlates of the vibrissae in the medullary trigeminal complex of the mouse. *Brain Res* 306: 374–379, 1984.

Nunez A and Buno W. In vitro electrophysiological properties of rat dorsal column nuclei neurons. *Eur J Neurosci* 11: 1865–1876, 1999.

Paxinos G and Watson C. *The Rat Brain in Stereotaxic Coordinates.* San Diego, CA: Academic Press, 1998.

Pellegrino LJ, Pellegrino AS, and Cushman AJ. *A Stereotaxic Atlas of the Rat Brain.* New York: Plenum Press, 1979.

Peschanski M. Trigeminal afferents to the diencephalon in the rat. *Neuroscience* 12: 465–487, 1984.

Poggio GF and Mountcastle VB. The functional properties of ventrobasal thalamic neurones studied in unanesthetized monkeys. *J Neurophysiol* 26: 775–806, 1963.

Powell TPS and Mountcastle VB. Some aspects of the functional organization of the cortex of the postcentral gyrus of the monkey: a correlation of findings obtained in a single unit analysis with cytoarchitecture. *Johns Hopk Hosp Bull* 105: 133–162, 1959.

Rhoades RW, Belford GR, and Killackey HP. Receptive-field properties of rat ventral posterior medial neurons before and after selective kainic acid lesions of the trigeminal brain stem complex. *J Neurophysiol* 57: 1577–1600, 1987.

Rice FL, Mance A, and Munger BL. A comparative light microscopic analysis of the sensory innervation of the mystacial pad. I. Innervation of the vibrissal follicle-sinus complexes. *J Comp Neurol* 252: 154–174, 1986.

Shipley MT. Response characteristics of single units in the rat's trigeminal nuclei to vibrissa displacements. *J Neurophysiol* 37: 73–90, 1974.

Shortland PJ, DeMaro JA, and Jacquin MF. Trigeminal structure-function relationships: a reevaluation based on long-range staining of a large sample of brainstem Aβ fibers. *Somatosensory Mot Res* 12: 249–275, 1995.

Shortland PJ, DeMaro JA, Shang F, Waite PME, and Jacquin MF. Peripheral and central predictors of whisker afferent morphology in the rat brainstem. *J Comp Neurol* 375: 481–501, 1996.

Shoykhet M, Doherty D, and Simons DJ. Coding of deflection velocity and amplitude by whisker primary afferent neurons: implications for higher level processing. *Somatosensory Mot Res* 17: 171–180, 2000.

Sikich L, Woolsey TA, and Johnson EM Jr. Effect of a uniform partial denervation of the periphery on the peripheral and central vibrissal system in guinea pigs. *J Neurosci* 6: 1227–1240, 1986.

Simons DJ. Multi-whisker stimulation and its effects on vibrissa units in rat SmI barrel cortex. *Brain Res* 276: 178–182, 1983.

Simons DJ. Temporal and spatial integration in the rat SI vibrissa cortex. *J Neurophysiol* 54: 615–635, 1985.

Simons DJ. Neuronal integration in the somatosensory whisker/barrel cortex. In: *Cerebral Cortex*, edited Jones EG and Diamond IT. New York: Plenum Press, 1995, vol. 11, p. 263–297.

Simons DJ and Carvell GE. Thalamocortical response transformation in the rat vibrissa/barrel system. *J Neurophysiol* 61: 311–330, 1989.

Simons DJ, Carvell GE, Hershey AE, and Bryant DP. Responses of barrel cortex neurons in awake rats and effects of urethane anesthesia. *Exp Brain Res* 91: 259–272, 1992.

Simons DJ and Land PW. Angular sensitivities of SmI barrel neurons and the effects of fentanyl anesthesia. *Soc Neurosci Abstr* 11: 751, 1985.

Smith RL. The ascending fiber projections from the principal sensory trigeminal nucleus in the rat. *J Comp Neurol* 148: 423–446, 1973.

Sosnik R, Haidarliu S, and Ahissar E. Temporal frequency of whisker movement. I. Representations in brain stem and thalamus. *J Neurophysiol* 86: 339–353, 2001.

Takahashi K. Slow and fast groups of pyramidal tract cells and their respective membrane properties. *J Neurophysiol* 28: 908–924, 1965.

Veinante P and Deschênes M. Single- and multi-whisker channels in the ascending projections from the principal trigeminal nucleus in the rat. *J Neurosci* 19: 5085–5095, 1999.

Veinante P, Jacquin MF, and Deschênes M. Thalamic projections from the whisker-sensitive regions of the spinal trigeminal complex in the rat. *J Comp Neurol* 420: 233–243, 2000.

Williams MN, Zahm DS, and Jacquin MF. Differential foci and synaptic organization of the principal and spinal projections to the thalamus in rats. *Eur J Neurosci* 6: 429–453, 1994.

Xiang C, Korutz A, Dong HX, Shen D, Arends J, and Jacquin MF. Circuits engaged by primary afferent terminals in the mouse trigeminal nucleus principalis. *Soc Neurosci Abstr* 26: 430, 2000.

Zucker E and Welker WI. Coding of somatic sensory input by vibrissal neurons in the rat's trigeminal ganglion. *Brain Res* 12: 138–156, 1969.